Advance in structural materials science
using synchrotron light, neutron, and muon

Comments
- High-T_c superconductivity -

Discussion Leader
Jun Akimitsu

Department of Physics and Mathematics,
Aoyama Gakuin University

Akimitsu Lab. HP
URL http://www.phys.aoyama.ac.jp/~w3-jun/

High Tc Superconductivity

- Spatial Correlation in the Vortex Matter Systems

  Steve Lee

- Challenging Experiments for Cuprate Superconductors

  Kazuyoshi Yamada

- Angle-resolved Photoemission Spectroscopy of High-Tc Superconductors: Present Status and Outlook

  Atsushi Fujimori

Introduction

- Most attractive word in the Physics Society is

  "Deep"

- On the other hand, in the Chemistry Society is

  "New"

↓

"Deep Physics" through "New Material"

Triangle Phase Diagram

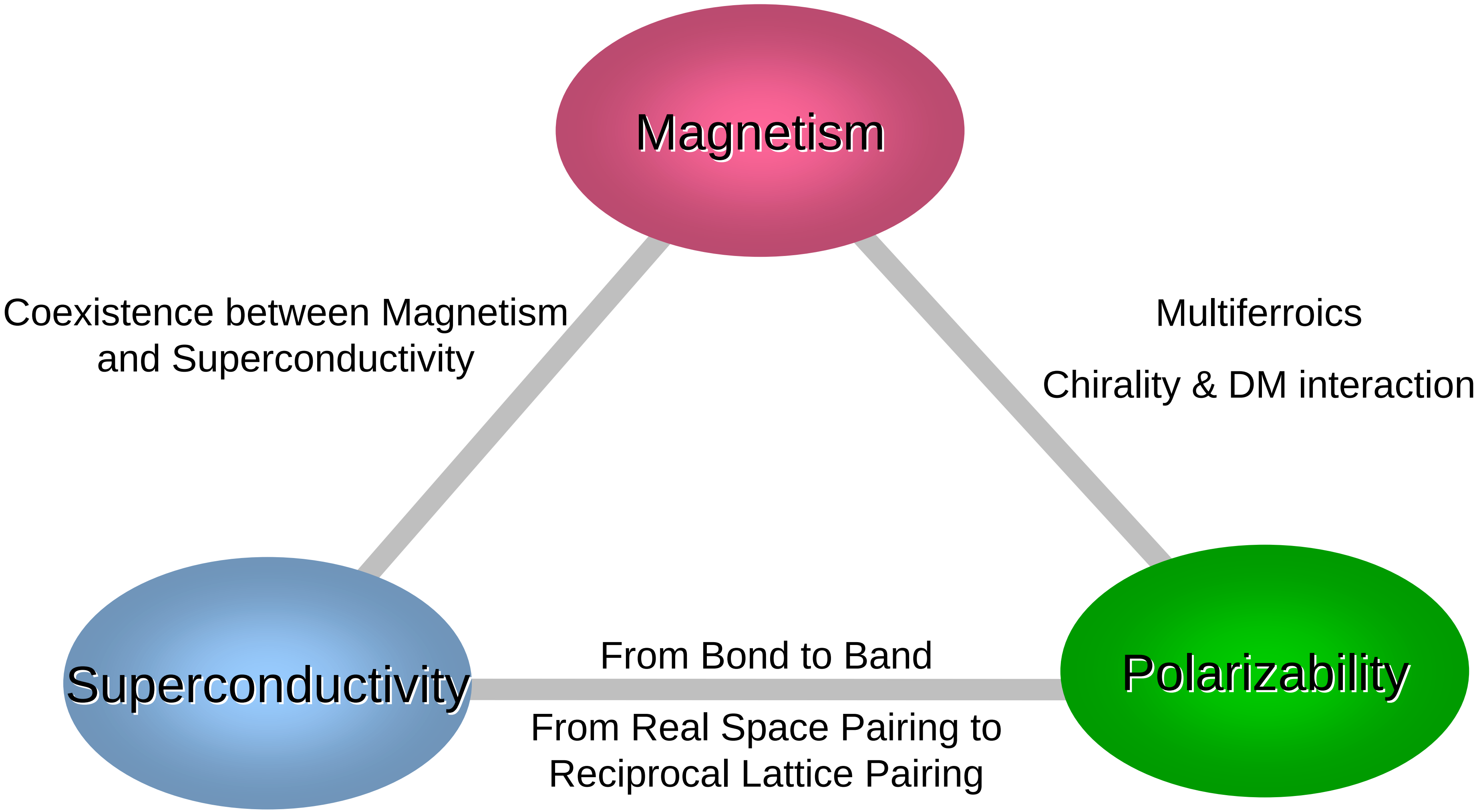

Phase Diagram

Chiral Helimagnetism

- Symmetric helix
  - No difference between right-handed and left handed screws

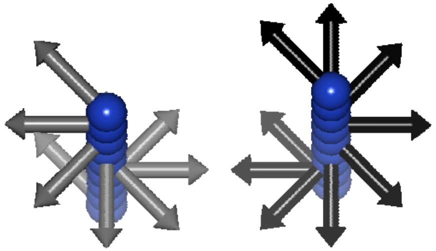

Dy, Ho

- (Ferro)chiral helix
  - Only right- (or left-) handed screws

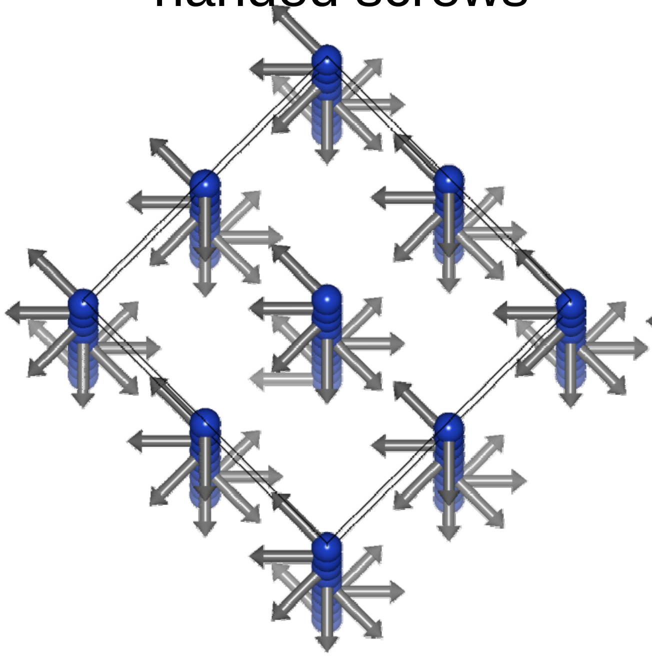

MnSi, $CsCuCl_3$ (?)

- (Antiferro)chiral helix
  - Alternating right-handed and left-handed screws

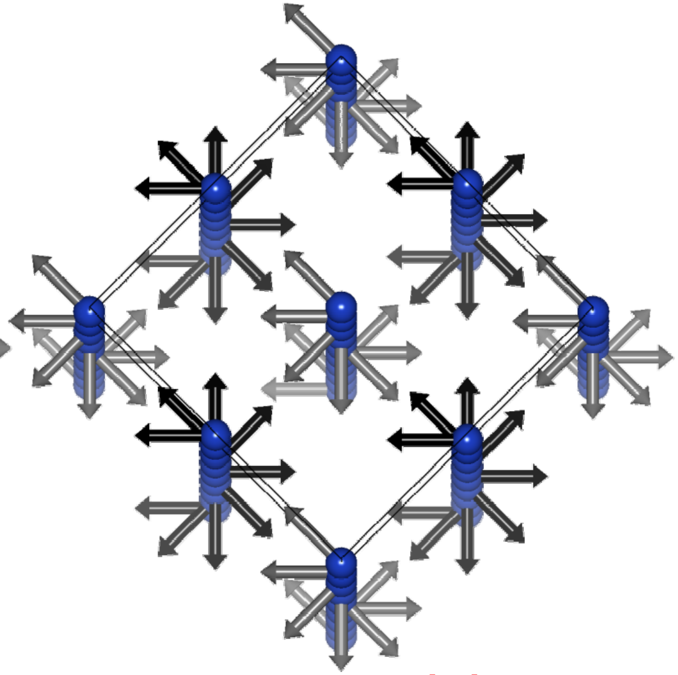

CuB_2O_4 (?)

Chirality of $CsCuCl_3$

- Determination of Crystallographic and Magnetic Chirality in $CsCuCl_3$
  - Resonant Circularly-polarized X-ray Diffraction
  - Non-resonant Circularly-polarized X-ray Diffraction

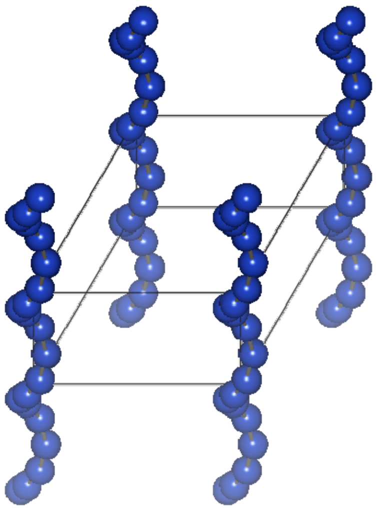

(Left-handed: $P6_122$)

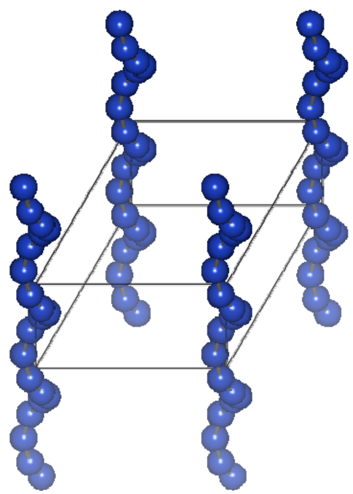

(Right-handed: $P6_522$)

Aoyama-Gakuin University

Resonat Circularly-polarized X-ray Diffraction

- Experimantal (@ BL19LXU, SPring-8)
  - Energy: 8.996 keV (Cu^{2+} *K*-edge)
  - T = Room temperature
  - Sample with SG: $P6_122$ and $P6_522$
    - Crystallographic chirality was determined by X-ray oscillation photograph

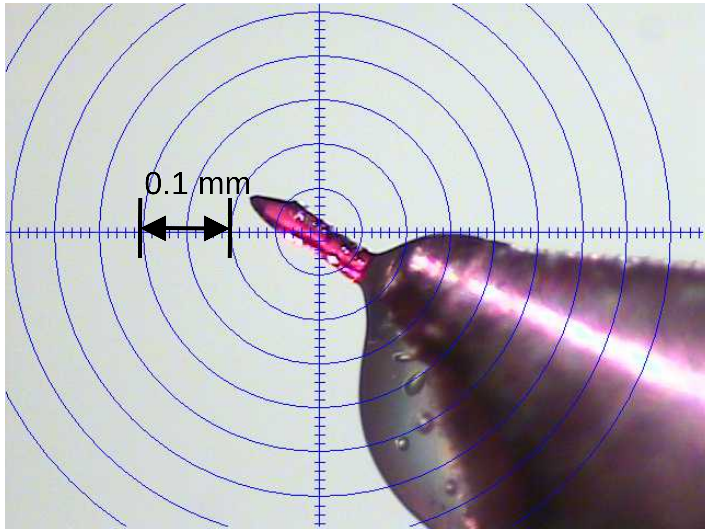

Resonat Circularly-polarized X-ray Diffraction

- Reciprocal lattice scan with $P6_122$ sample

(0,0,10)

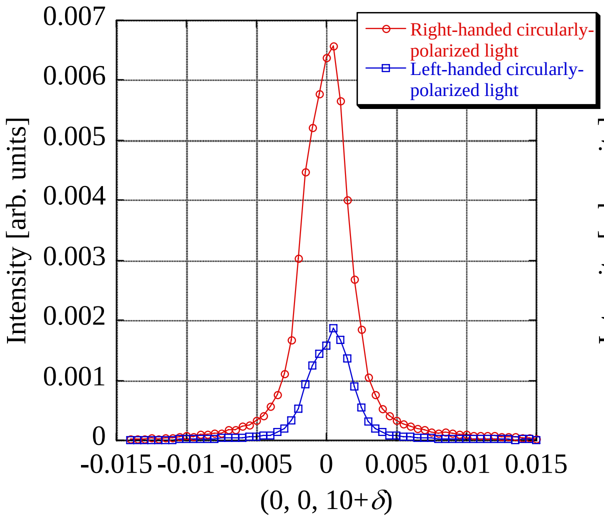

(0,0,12)

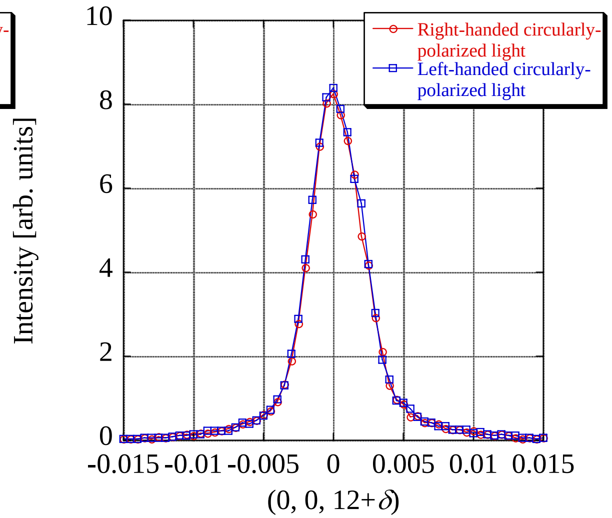

(0,0,14)

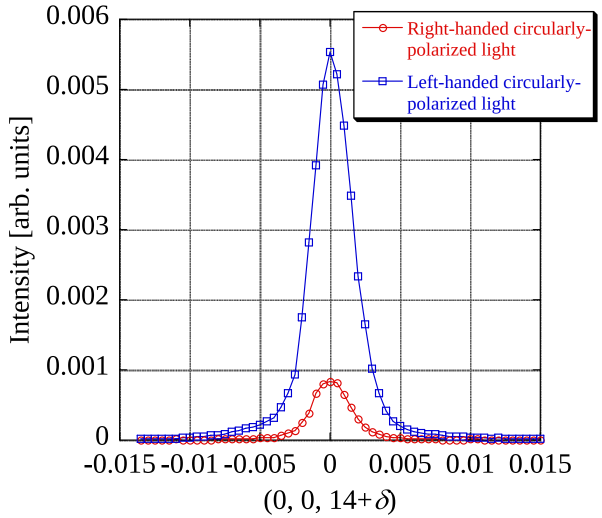

Intensities in (0,0,6n±2) are flipped by the change of circular polarization

Aoyama-Gakuin University

Resonat Circularly-polarized X-ray Diffraction

- Reciprocal lattice scan with $P6_522$ sample

(0,0,10)

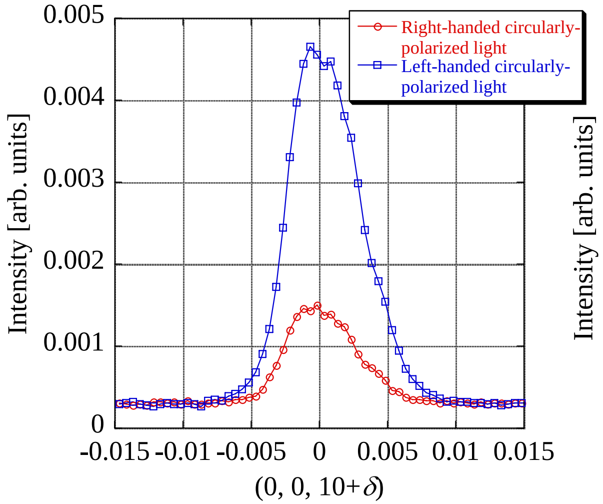

(0,0,12)

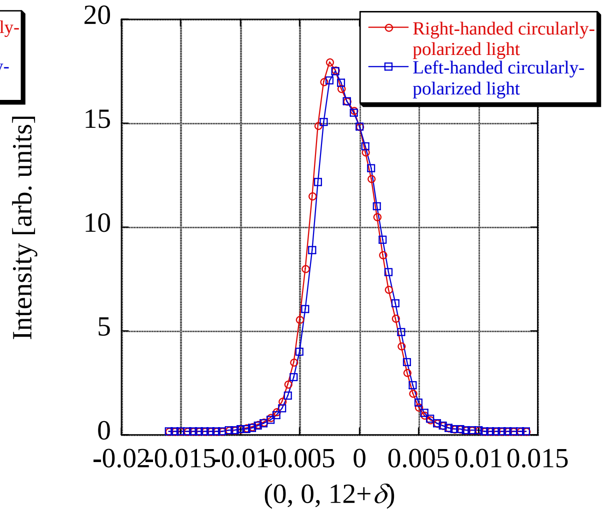

(0,0,14)

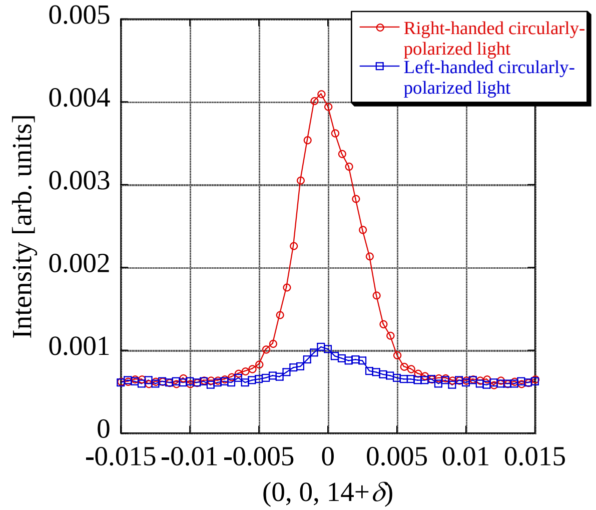

Intensities in (0,0,6n±2) are flipped by the change of crystallographic chirality

Aoyama-Gakuin University

Phase Diagram

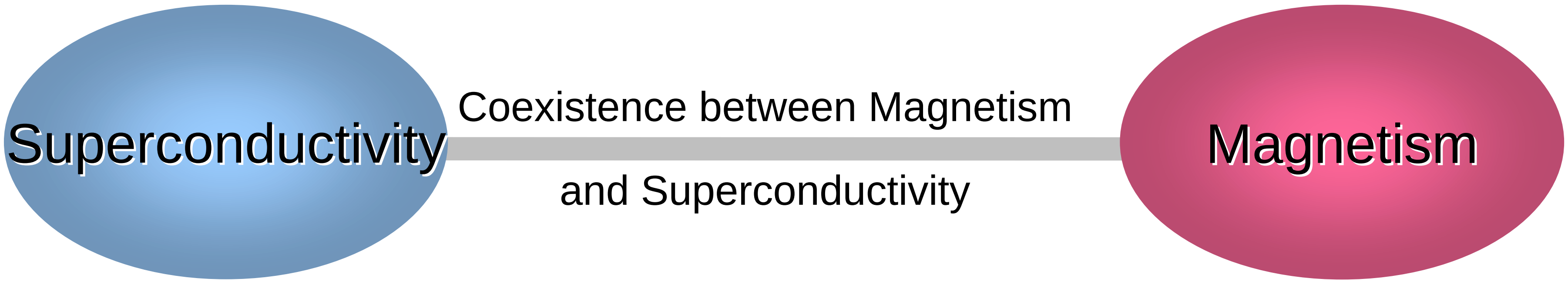

Coexistence between superconductivity and magnetism

Hg-1245 system

(T_c=108K; 5-CuO_2 plane)

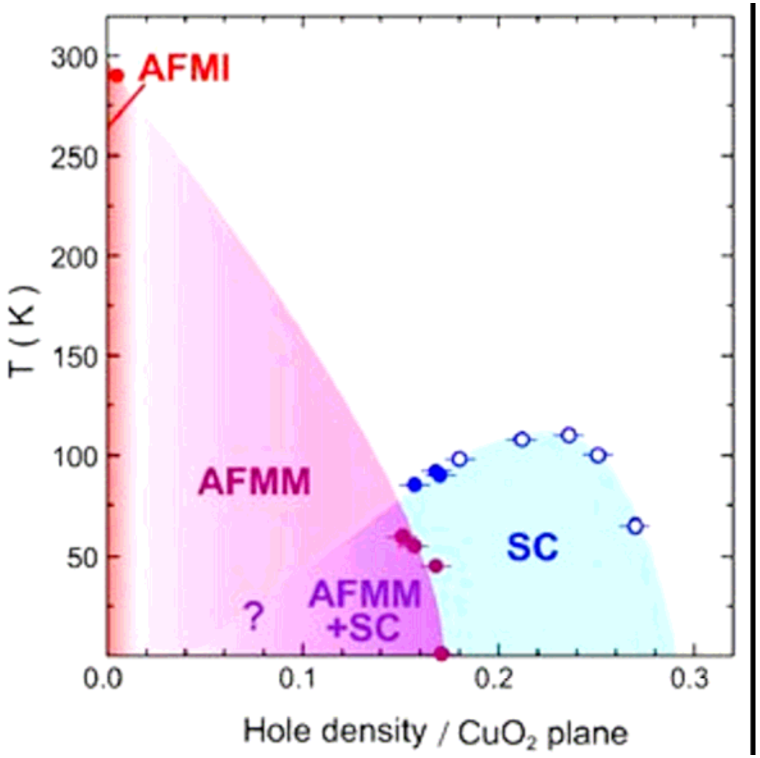

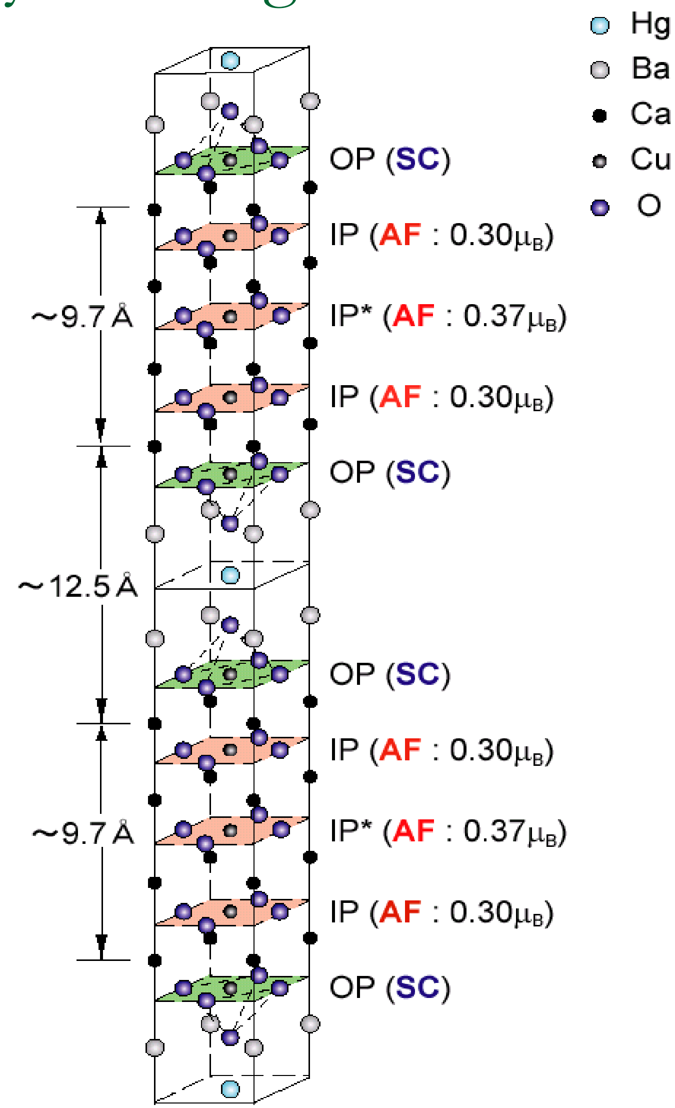

By Kitaoka group

Aoyama-Gakuin University

Coexistence between superconductivity and magnetism

$Tm_5Rh_6Sn_{18}$

Single crystal

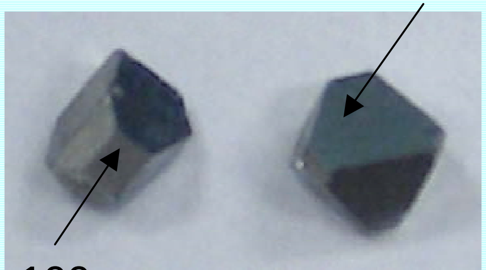

Crystal size; 3×3×5mm

By Naoki Kase (DC2)

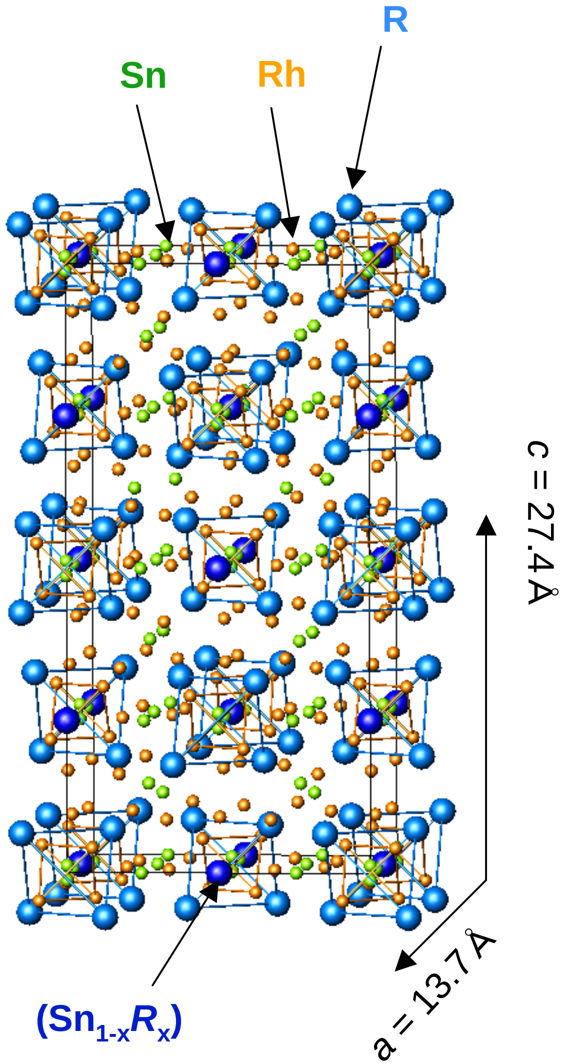

Coexistence between superconductivity and magnetism

Resistivity under magnetic fields and H-T phase diagram in $Tm_5Rh_6Sn_{18}$

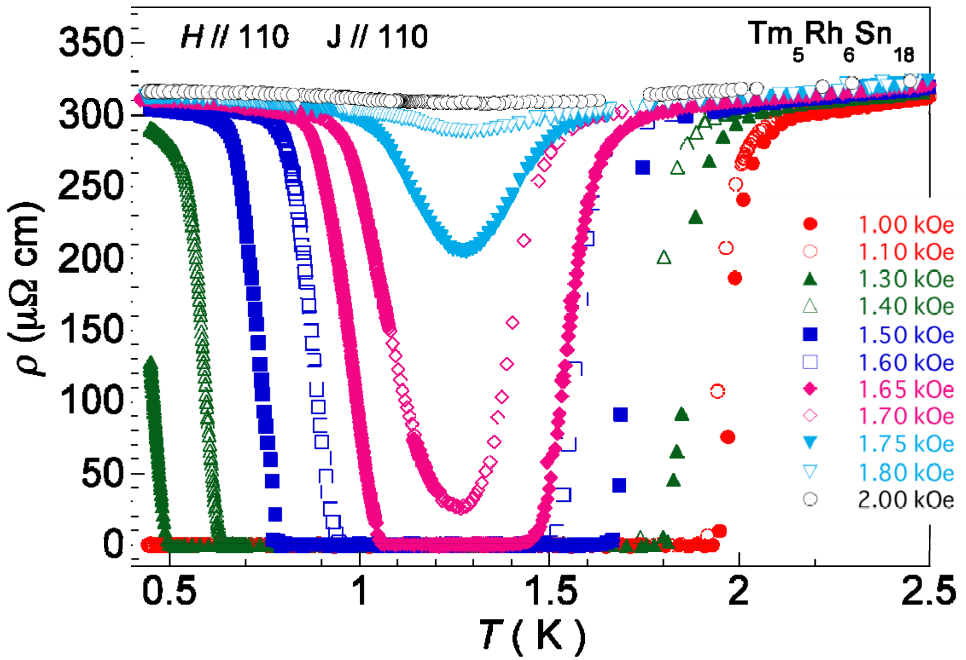

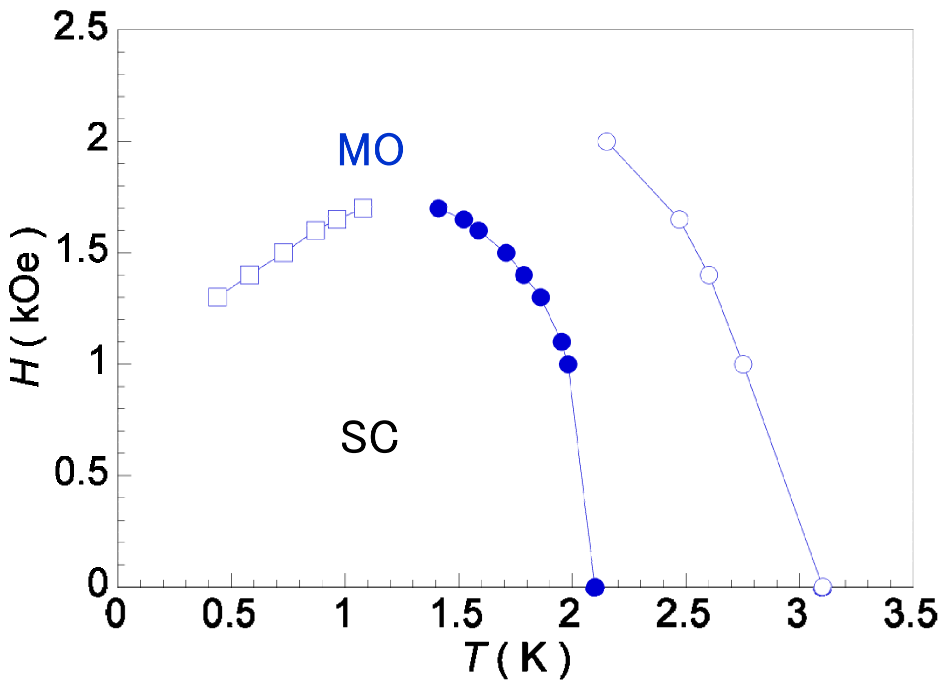

"Reentrant superconductivity" was observed at low temperature.

mSR measurement

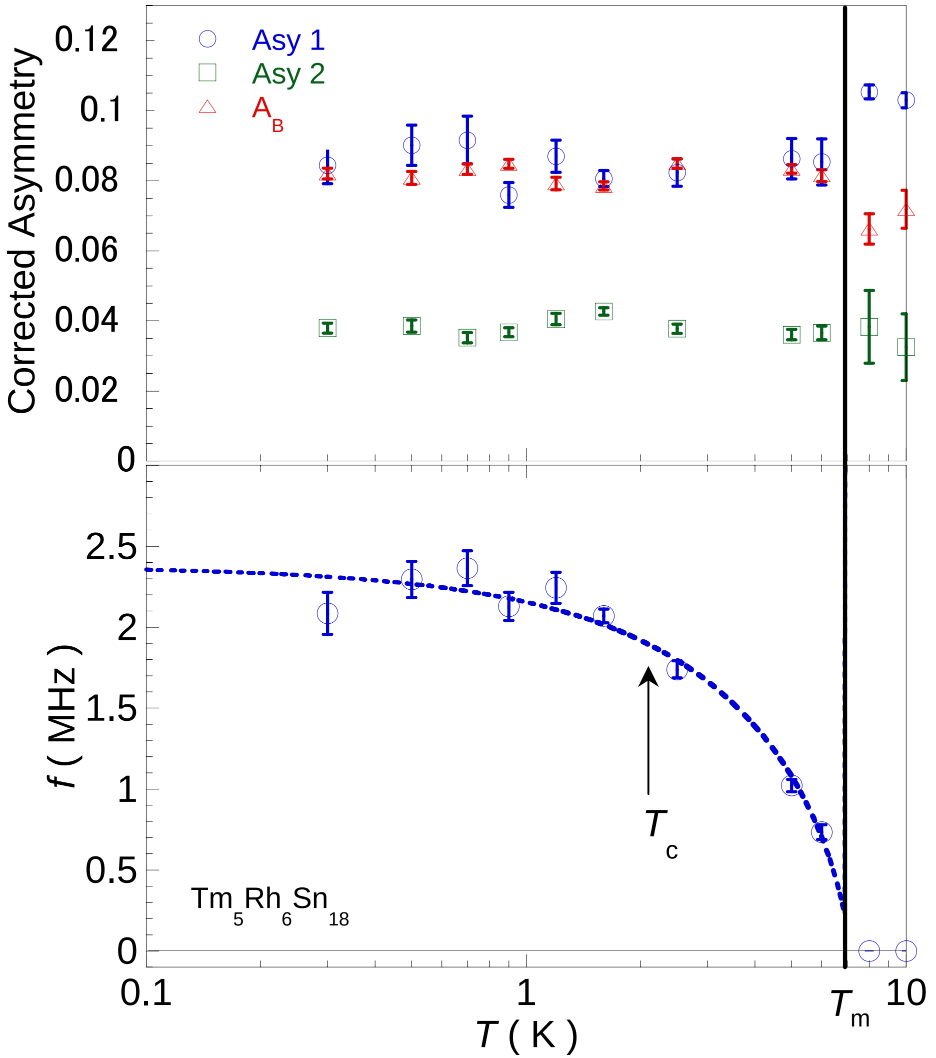

Fitting function

$$A_1 \exp(-\lambda_1 t)\cos(f t + \delta) + A_2 \exp(-\lambda_2 t) + A_B$$

$A_1/(A_1 + A_2) = 0.67$

Magnetic Volume Function is ~100 %

$f = f(0)(1 - T/T_m)^{\beta}$ $f = \gamma H$

Internal magnetic field, H = 170 Oe

T_m = 6.7 K

T_m is corresponding to T_M obtained from specific heat measurement.

Superconductivity in $(Y,Tm)_5Rh_6Sn_{18}$

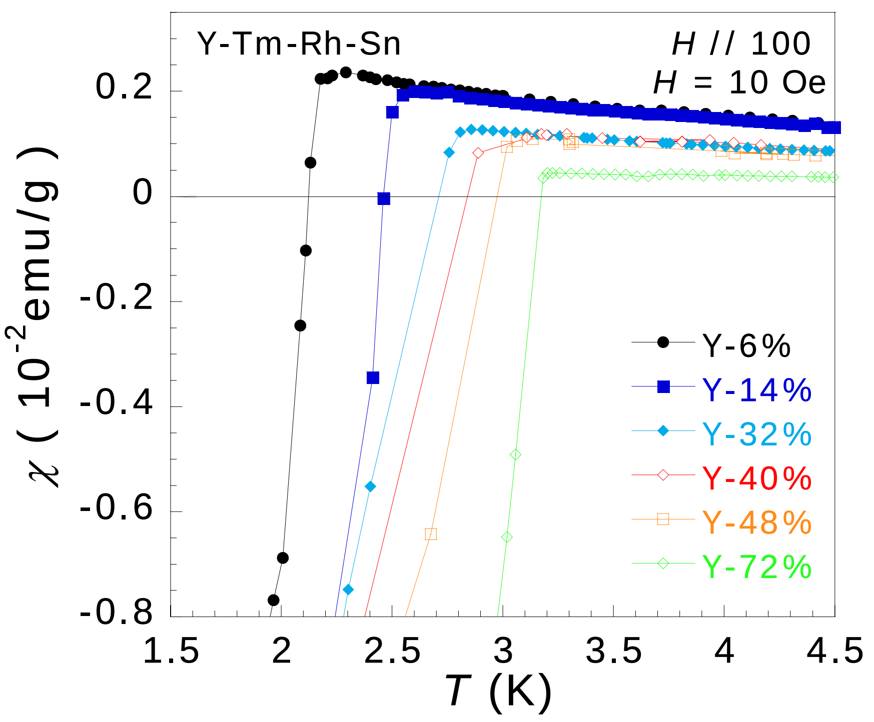

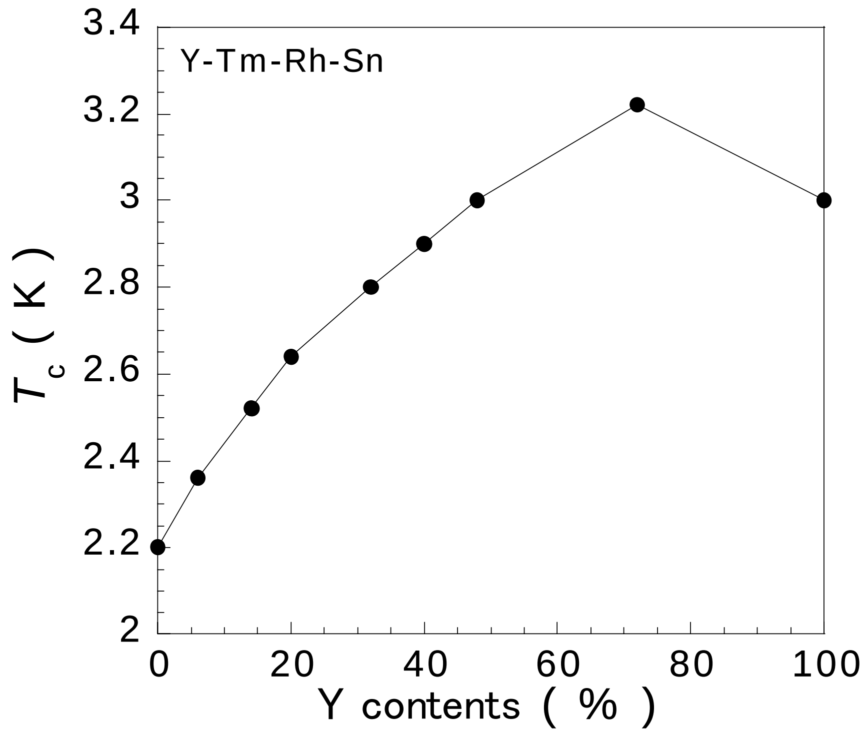

- T_c is changed by Y-doping to Tm site.

H-T phase diagrams of $(Y,Tm)_5Rh_6Sn_{18}$

- By Y-doping
  - The region of SC is enlarged.
  - Reentrant SC state is disappeared at 32% doping.

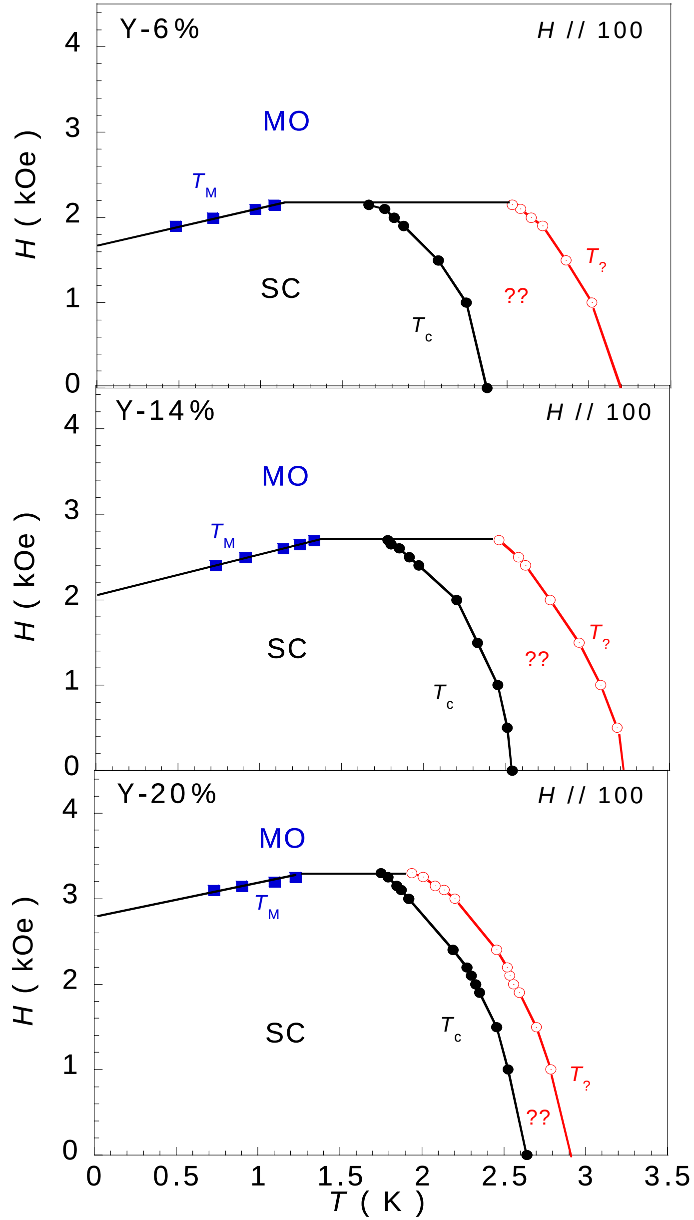

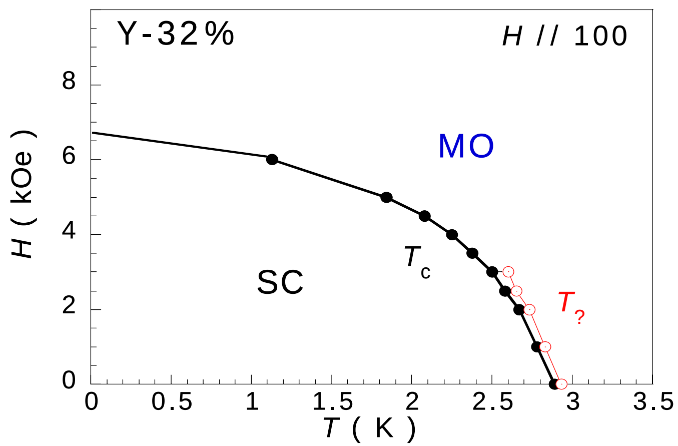

Aoyama-Gakuin University

Phase Diagram

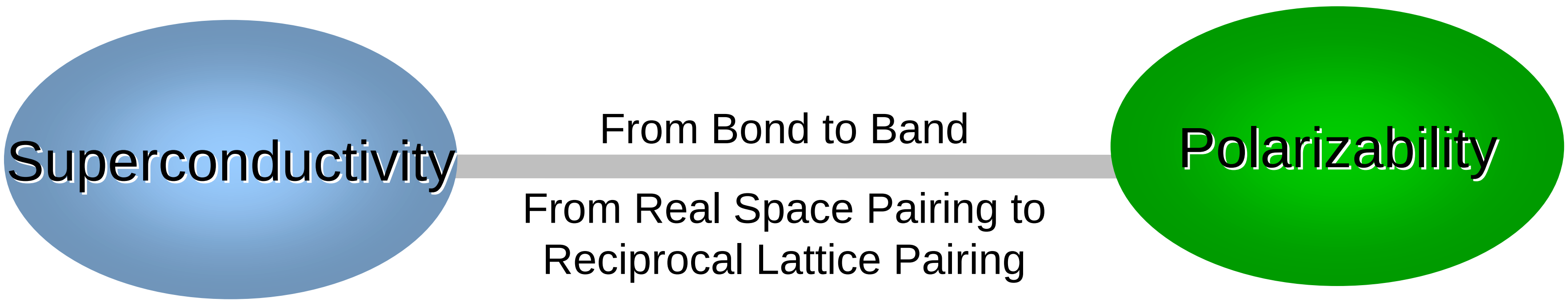

From bond to band (by H. Fukuyama)

Superconductivity in B-doped diamond, SiC and MgB_2.

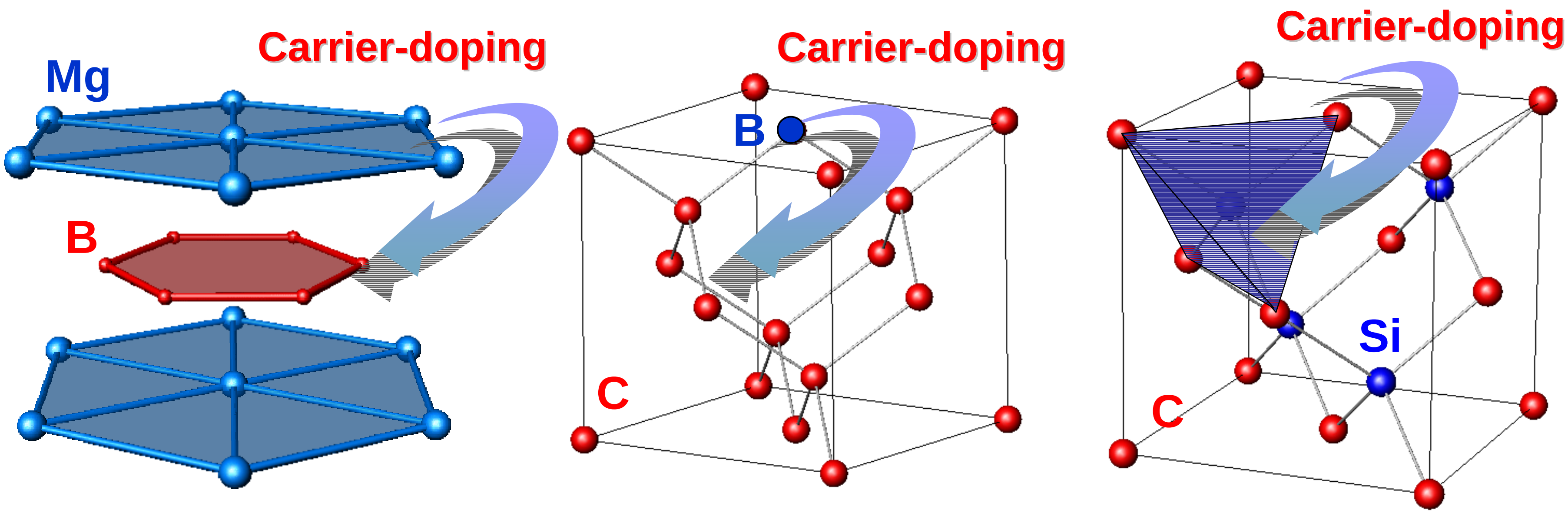

MgB_2 Diamond SiC

Covalent bonds become bands by carrier-doping.

Superconductivity in B-doped SiC

- T_c~1.4K
  - ΔT_c: 0.15K
- Hole carrier
  - 1.06-1.91×10^{21} cm^{-3}
  - B-substitution is 2.2-3.9 at%

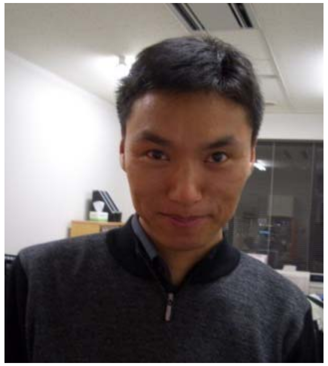

Z.-A. Ren

T. Muranaka

- Type-I SC state
  - No T-hysteresis was observed under zero field.
  - The degree of T-hysteresis was enhanced with decreasing temperature.
  - H_c=115Oe(S→N), H_{SC}=85Oe(N→S)

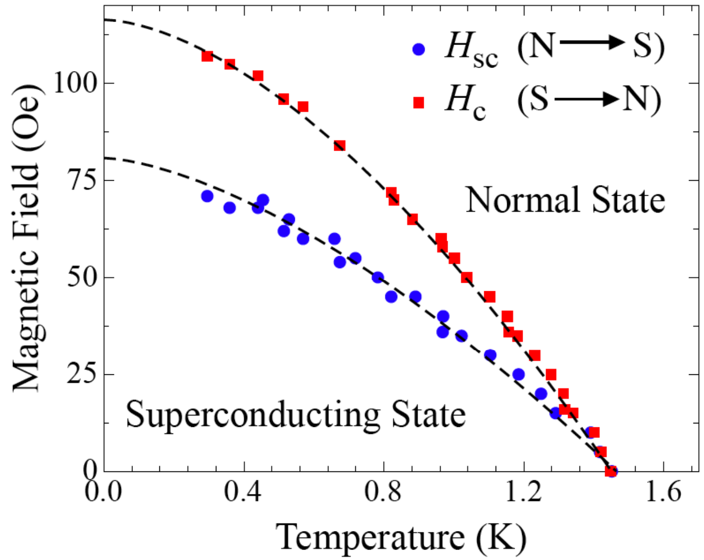

Z.-A. Ren *et al.*, JPSJ 76(10), 103710 (2007).

Aoyama-Gakuin University

Crystal structure of Ag_6O_8MX

The silver-oxide Ag_6O_8MX (M = cation, X = anion) has a clathrate-type structure which consists of face sharing Ag_6O_8 cage containing anion (X^-) at its center.

K. Kawashima

- $Ag_6O_8AgNO_3$ (T_c=1.04 K)
- $Ag_6O_8AgBF_4$ (T_c=0.35 K)
- $Ag_6O_8AgHF_2$ (T_c=0.15~1.5 K)
- $Ag_6O_8AgHSO_4$
- $Ag_6O_8AgHCO_3$
- $Ag_6O_8AgClO_4$

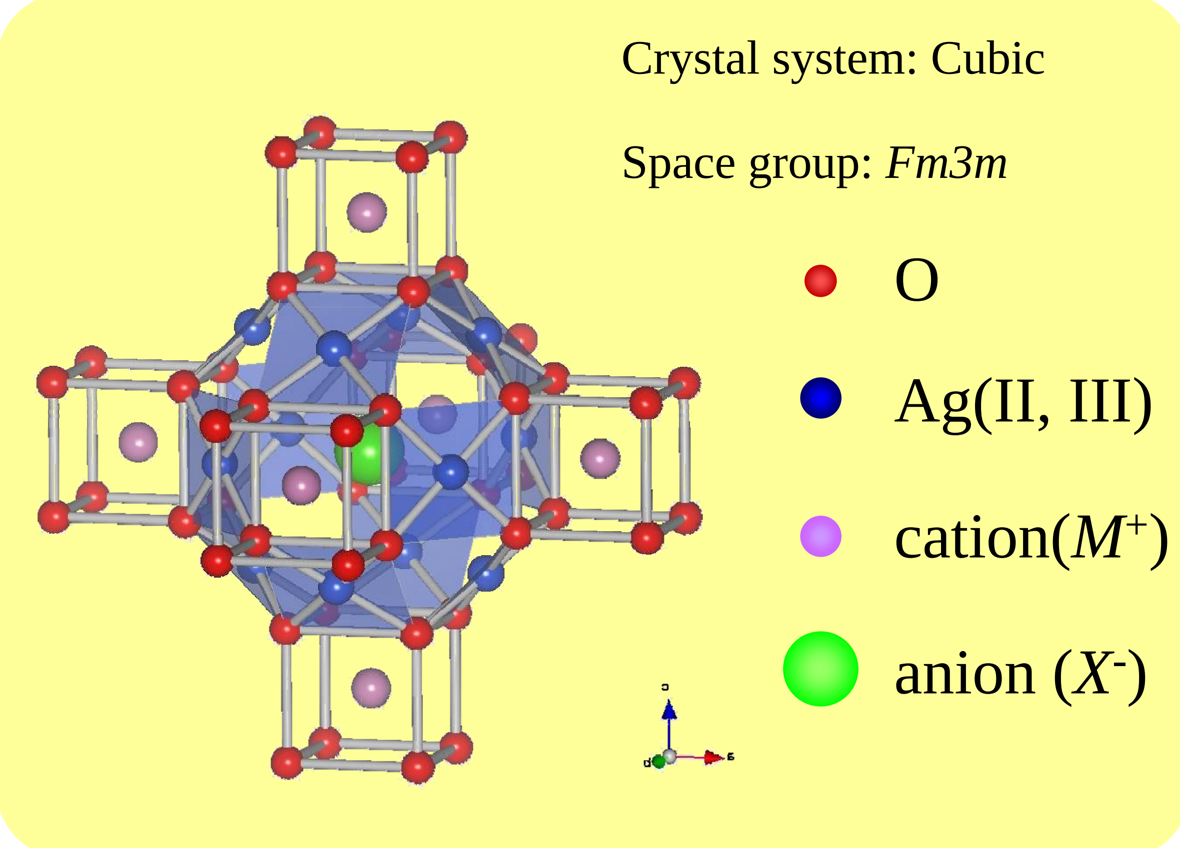

[1] J. Selbin *et al*., J. Inorg. Nucl. Chem., **20** (1961) 91.
[2] M. B. Robin *et al*., Phys. Rev. Lett. **17** (1966) 917.
[3] M. Jansen *et al*., J. Alloys and Compounds **183** (1992) 45.

Normal state of $Ag_6O_8AgNO_3$ and $Ag_6O_8AgHF_2$

$Ag_6O_8AgNO_3$

$Ag_6O_8AgNO_3$ shows phase transitions near 90 K and 180 K.

180 K: Structural phase-transition from Cubic to Tetragonal.

(We confirmed this transition using X-ray diffraction).

90 K: Small phase transition: stopping of NO_3^- ions rotation?

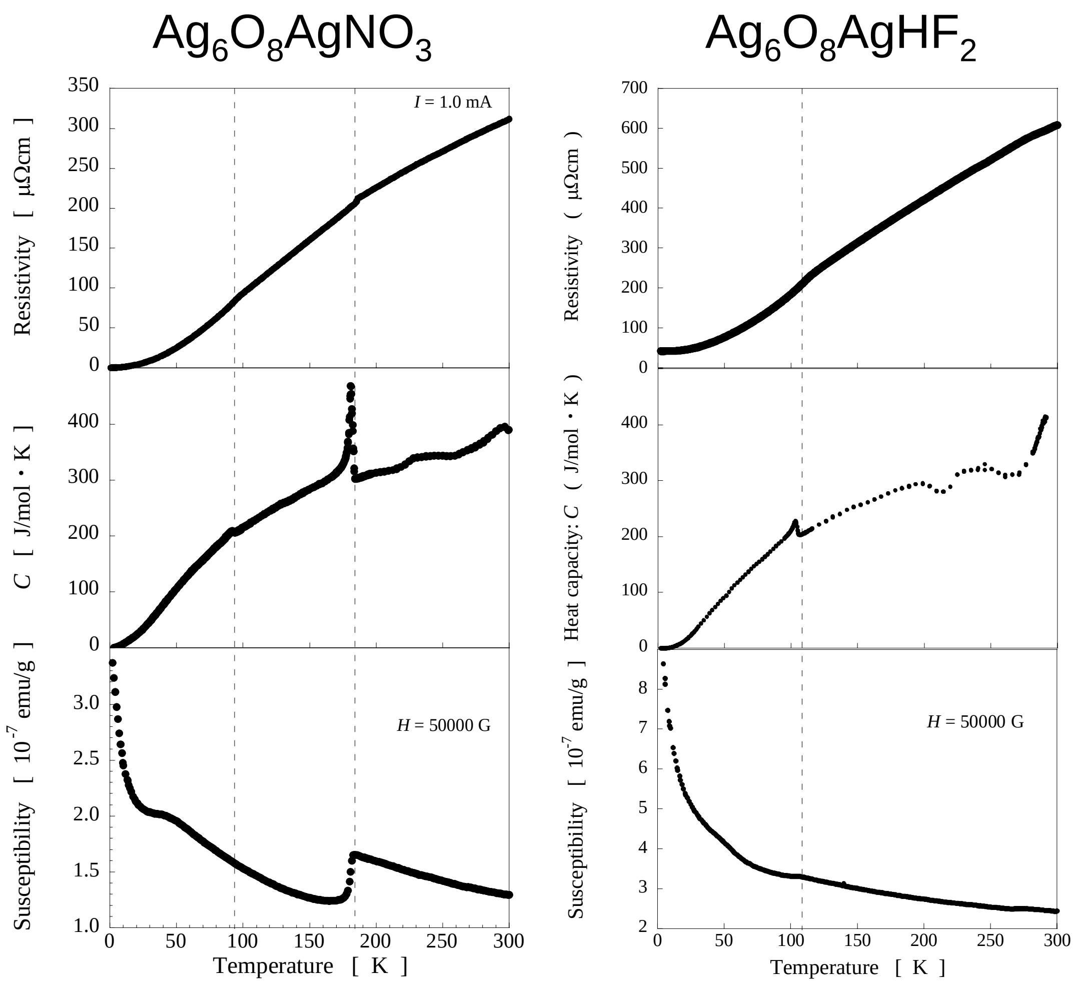

$Ag_6O_8AgHF_2$

$Ag_6O_8AgHF_2$ shows phase transition near 110 K. We consider that this transition is generated by stop of HF2- ions spin like $Ag_6O_8AgNO_3$ material.

Aoyama-Gakuin University

Superconducting state of $Ag_6O_8AgNO_3$ and $Ag_6O_8AgHF_2$

$Ag_6O_8AgNO_3$

$Ag_6O_8AgNO_3$ shows superconducting transition at 1.04 K as described in a previous report. We determine a upper critical field: H_{c2} to be 770 Oe and calculated coherence length: ζ to be 42.5 nm.

Resistivity & heat capacity.

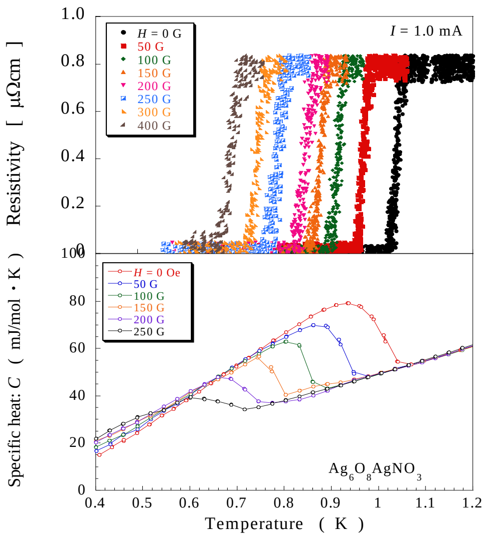

ac-susceptibility.

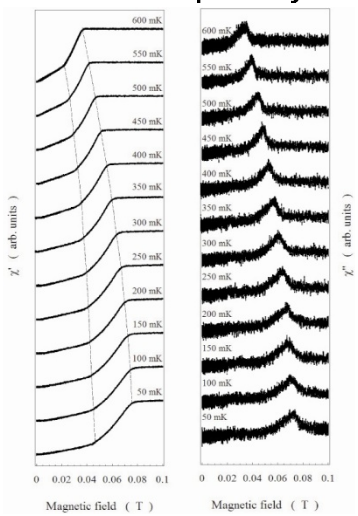

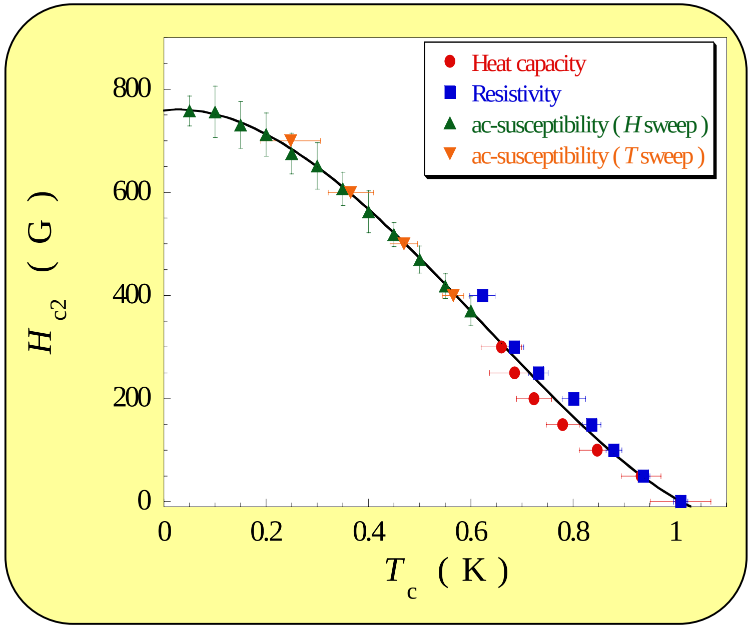

$Ag_6O_8AgHF_2$

We confirmed superconducting transition at 1.5 K more clear than previous report and performed some measurements to elucidate superconducting state in $Ag_6O_8AgHF_2$.

Aoyama-Gakuin University

Conclusion

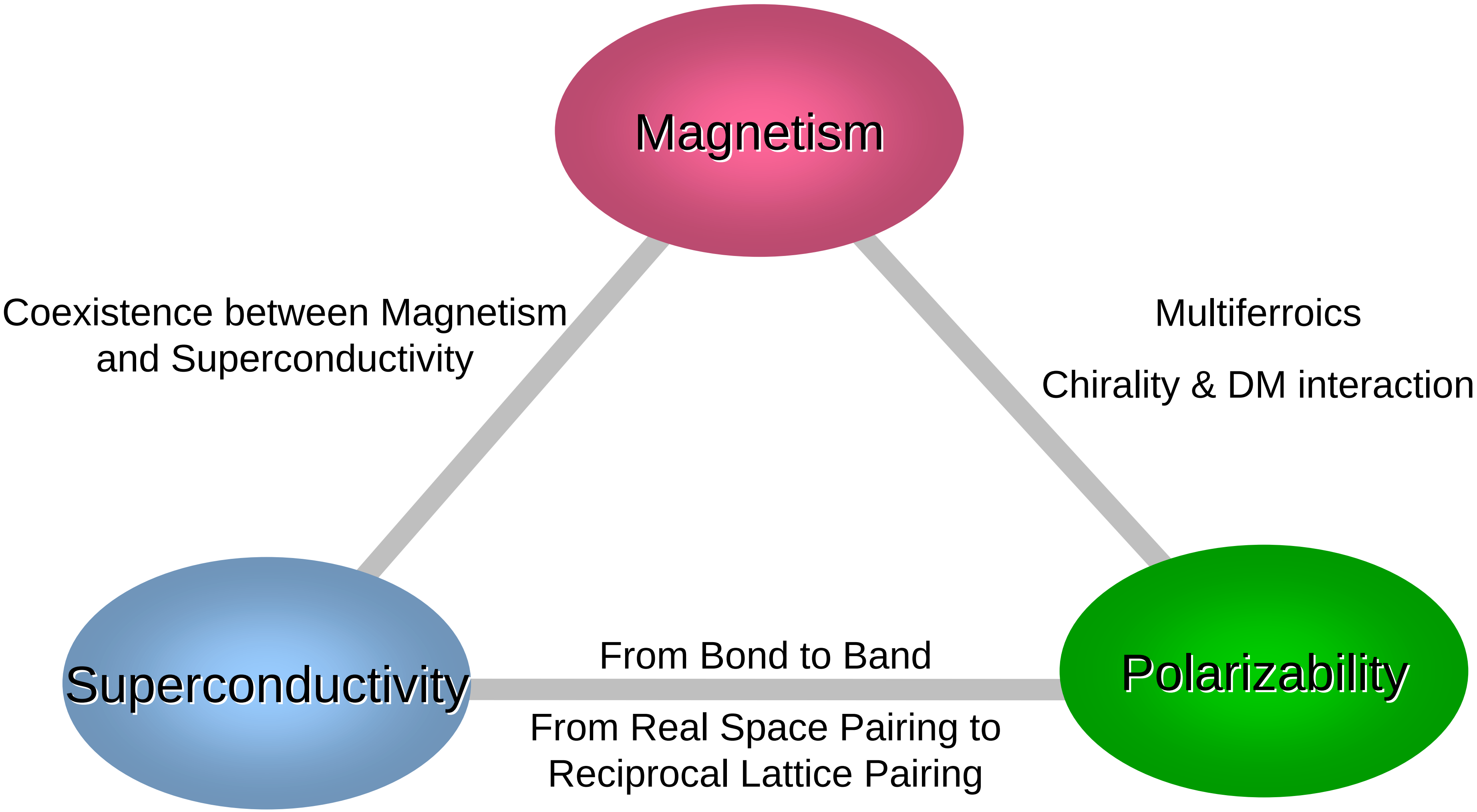
Magnetism
Coexistence between Magnetism and Superconductivity
Multiferroics
Chirality & DM interaction
Superconductivity
From Bond to Band
From Real Space Pairing to Reciprocal Lattice Pairing
Polarizability

Conclusion

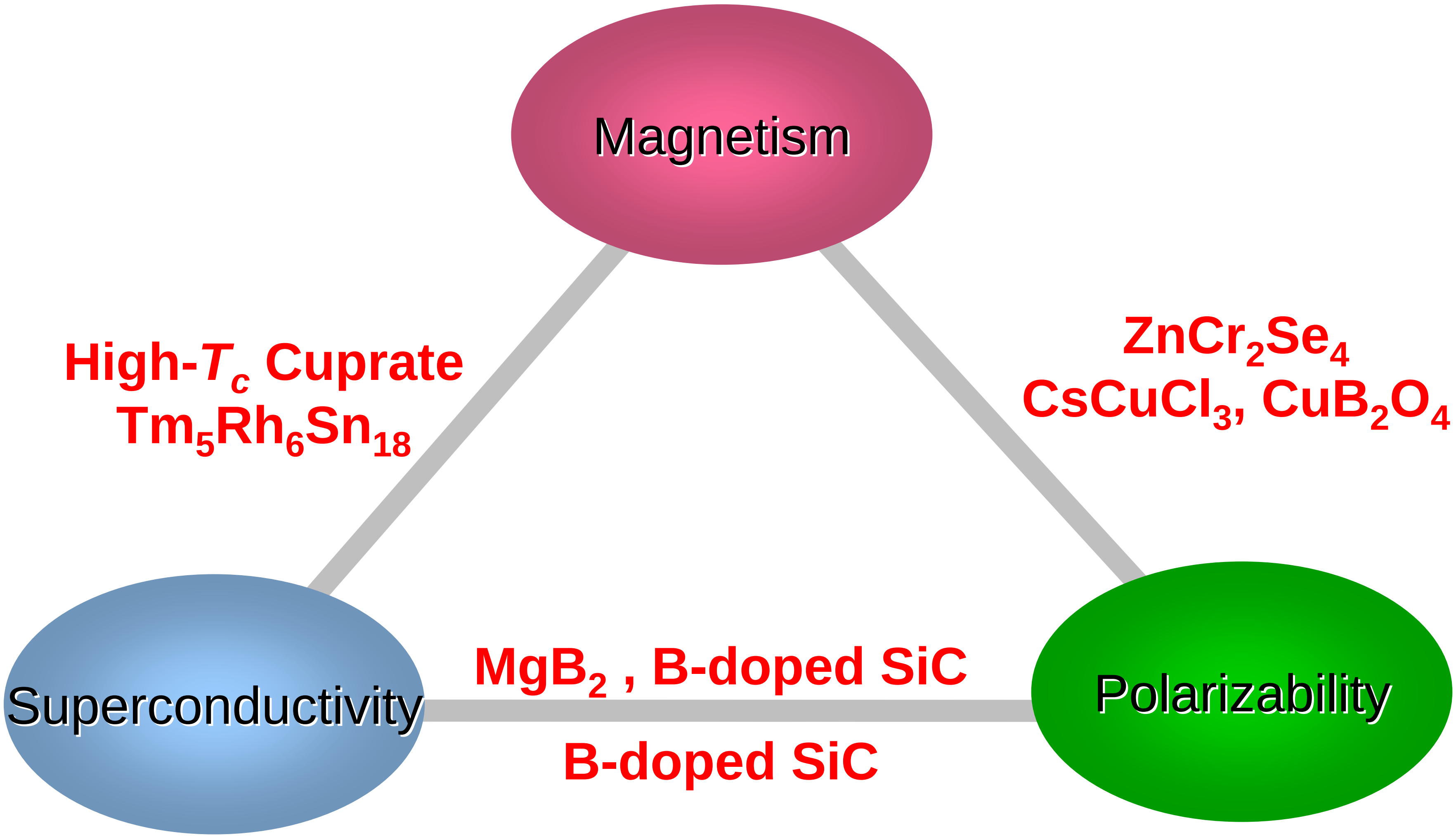
Magnetism
Superconductivity
Polarizability
High-T_c Cuprate
$Tm_5Rh_6Sn_{18}$
$ZnCr_2Se_4$
$CsCuCl_3$, CuB_2O_4
MgB_2 , B-doped SiC
B-doped SiC

Multiferroics

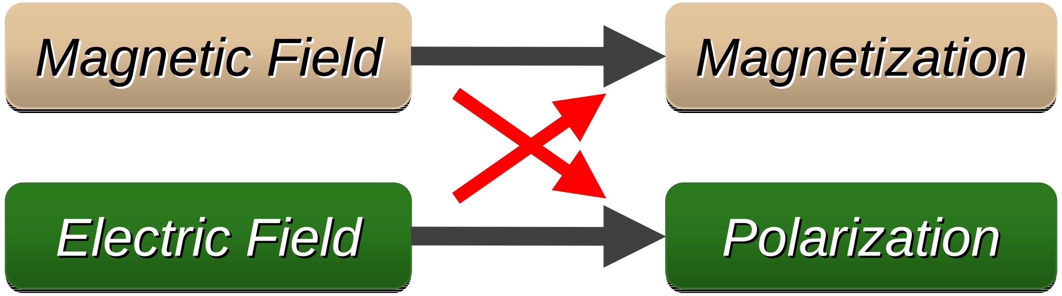

- $ZnCr_2Se_4$
  - Controling magnetic chiral domains with electric polarization

Polarized Neutron Diffraction

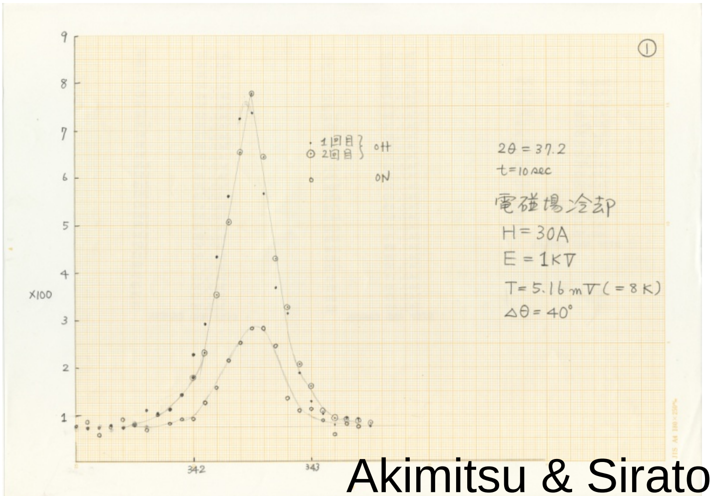

Akimitsu & Siratori

Inverse DM Interaction

$$P \propto Q \times (S_i \times S_{i+1})$$

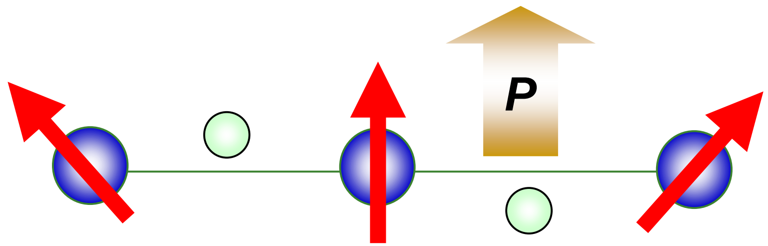

Katsura *et al.*

Aoyama-Gakuin University

Chirality & DM Interaction

Symmetric Helix

- No difference between right-handed and left handed screw

(Ferro)chiral Helix

- Only right (or left) handed screw

(Antiferro)chiral Helix

- Alternating right-handed and left-handed screw

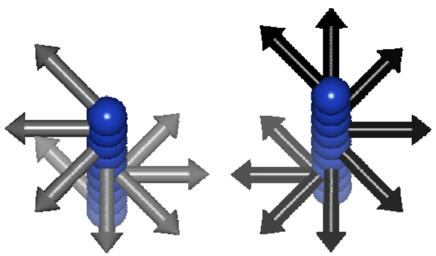

Dy, Ho

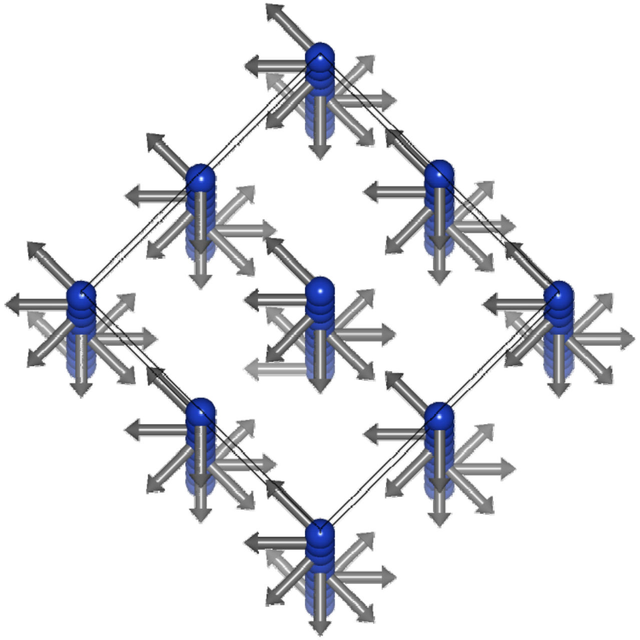

$CsCuCl_3$

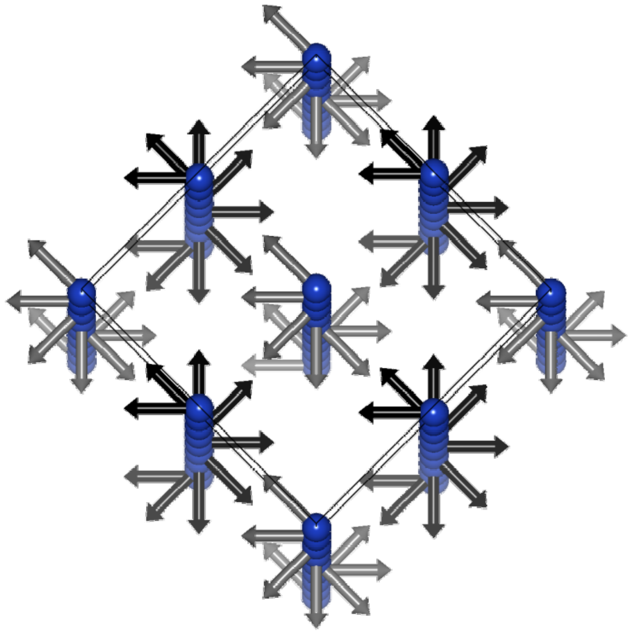

CuB_2O_4

Observation of Chirality

- Collaborators
  - Y. Kousaka, Y. Nakao, E. Kaya (Aoyama-Gakuin University)
  - S. Sakai (Hiroshima University)
  - H. Ohsumi, T. Komesu (RIKEN)
  - T. Arima (Tohoku University)

What is “Chirality” ?

- "I call any geometrical figure, or group of points, chiral, and say it has chirality, if its image in a plane mirror, ideally realized, cannot be brought to coincide with itself.“

Lord Kelvin (1904)

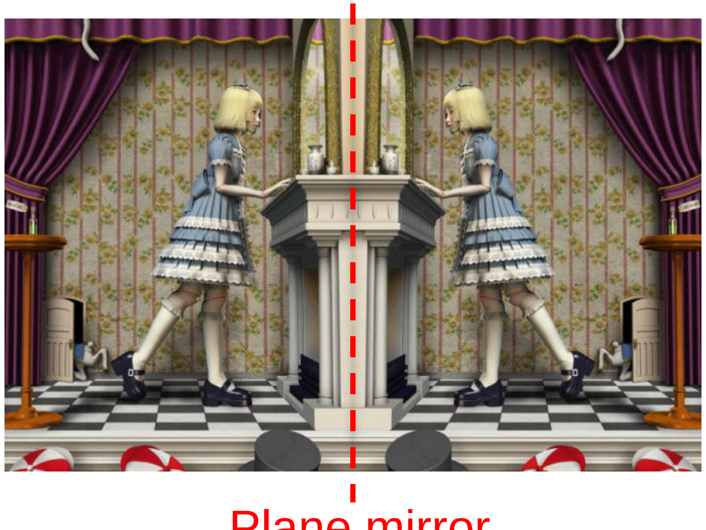

How to Observe Chiral Helimagnetism

- Polarized Neutron Diffraction Experiments
  - Magnetic scattering cross section

$$\left(\frac{d\sigma}{d\Omega}\right) = A|S|^2 \left[\begin{array}{l} \left\{1 + (Q\cdot q)^2 + 2(Q\cdot q)(P\cdot Q)\right\}\delta(Q = K - q) \\ + \left\{1 + (Q\cdot q)^2 - 2(Q\cdot q)(P\cdot Q)\right\}\delta(Q = K + q) \end{array} \right] \quad \begin{cases} Q & \text{: Scattering vector} \\ q & \text{: Magnetic propagation vector} \\ P & \text{: Neutron spin direction} \end{cases}$$

M. Blume *et al*.

  - Neutron spin P is parallel to Q

$$\left(\frac{d\sigma}{d\Omega}\right) = 4A|S|^2 \quad \text{at } Q = K\text{-}q$$

$$\left(\frac{d\sigma}{d\Omega}\right) = 0 \quad \text{at } Q = K\text{+}q$$

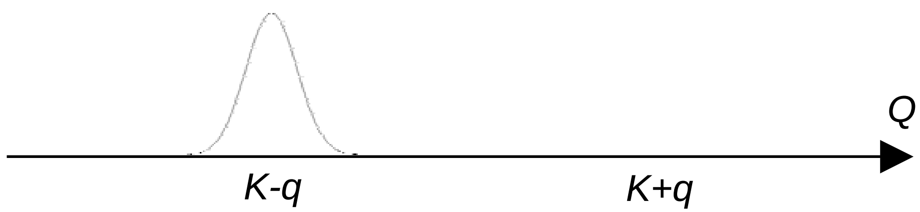

  - Neutron spin P is antiparallel to Q

$$\left(\frac{d\sigma}{d\Omega}\right) = 0 \quad \text{at } Q = K\text{-}q$$

$$\left(\frac{d\sigma}{d\Omega}\right) = 4A|S|^2 \quad \text{at } Q = K\text{+}q$$

How to Observe Chiral Helimagnetism

- Polarized Neutron Diffraction Experiments
  - Comparing magnetic satellite intensities between up-spin neutron and down-spin neutron
    - $ZnCr_2Se_4$
    - MnSi
    - $TbMnO_3$

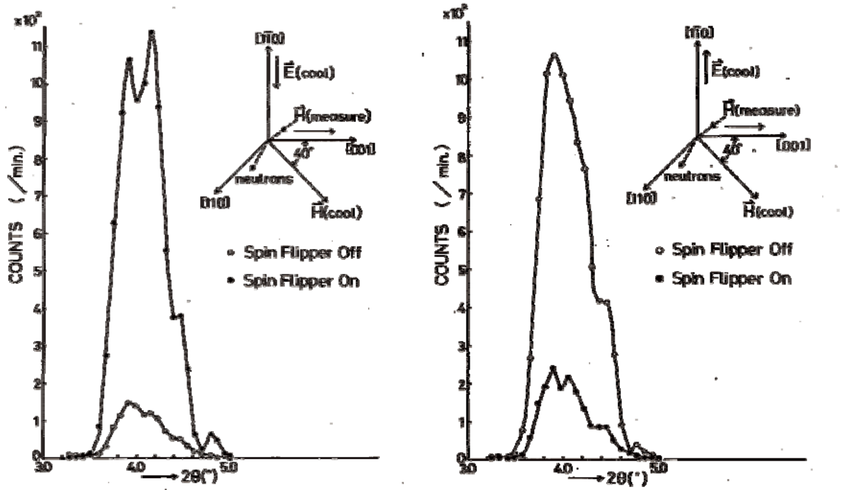

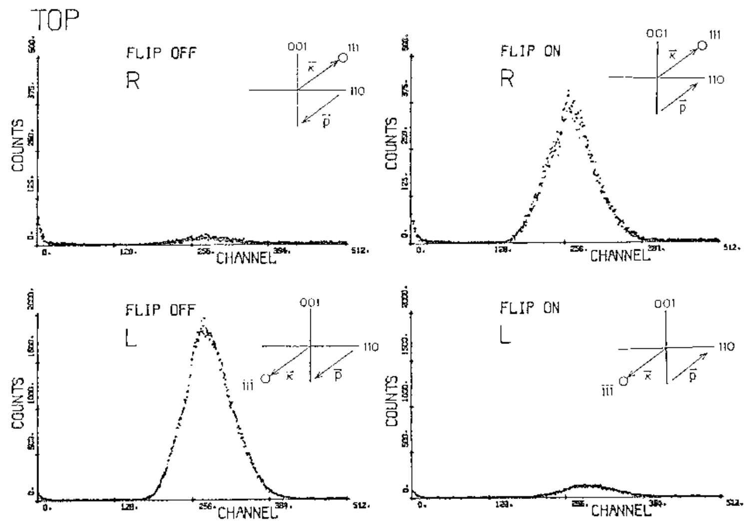

$ZnCr_2Se_4$, K. Siratori and J. Akimitsu *et al.*: J. Phys. Soc. Jpn. 48 (1980) 1111.

MnSi, M. Ishida *et al.*: J. Phys. Soc. Jpn. 54 (1985) 2975.

Circularly-polarized X-ray Diffraction

- Circularly-polarized X-ray Diffraction
  - New method to observe crystallographic and magnetic chirality
    - Crystallographic chirality can be determined by resonant X-ray diffraction method.
    - Magnetic chirality can be also detemined by non-resonant magnetic X-ray diffraction method
    - Circularly-polarization cannot be destroyed by an applied magnetic field

Circularly-polarized X-ray Diffraction

- Asymmetric Magnetic Satellites
  - Polarized Neutron Diffraction

$$\left(\frac{d\sigma}{d\Omega}\right) = A|S|^2 \left[\begin{array}{l} (1+P)\delta(Q=K-q) \\ +(1-P)\delta(Q=K+q) \end{array} \right]$$

  - Circularly-polarized X-ray Diffraction

$$\left(\frac{d\sigma}{d\Omega}\right) = A'|S|^2 \left[\begin{array}{l} \{(1+P\sin\theta)\sin\theta\cos\theta\}^2 \delta(Q=K-q) \\ +\{(1-P\sin\theta)\sin\theta\cos\theta\}^2 \delta(Q=K+q) \end{array} \right]$$

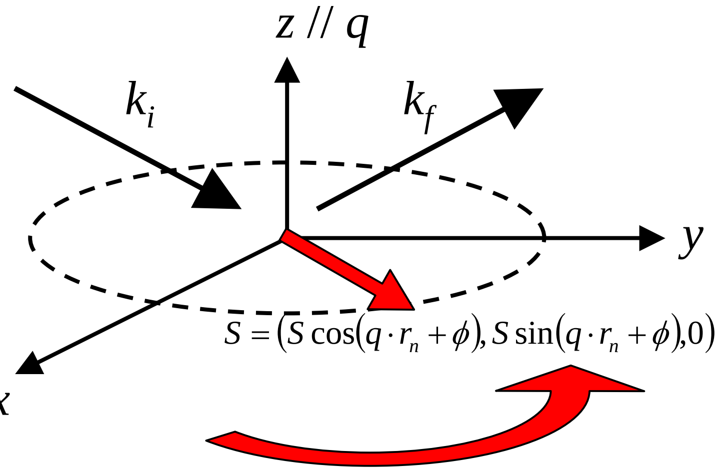

H. Ohsumi *et al.*: unpublished

- P = 1 (Up-spin or right-handed)

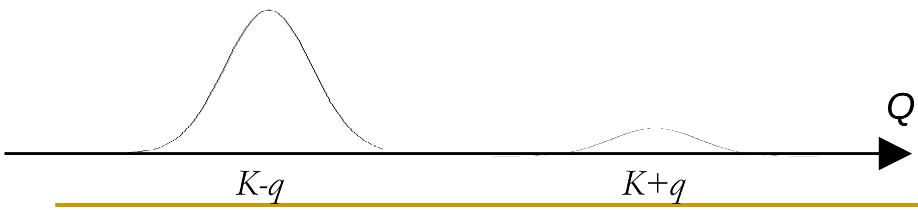

- P = -1 (Down-spin or left-handed)

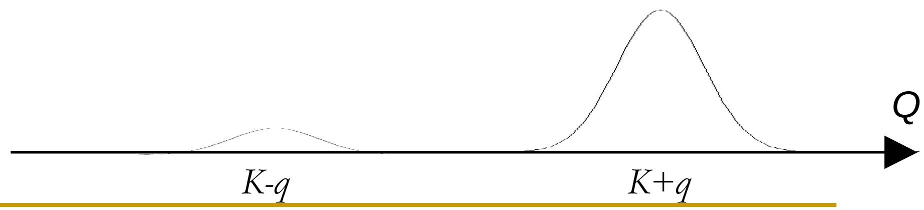

Introduction

- $CsCuCl_3$
  - Chiral Crystal Structure (SG: $P6_122$ or $P6_522$)
  - Helimagnetic Sturcutre along the *c*-axis (T < 10.5 K)

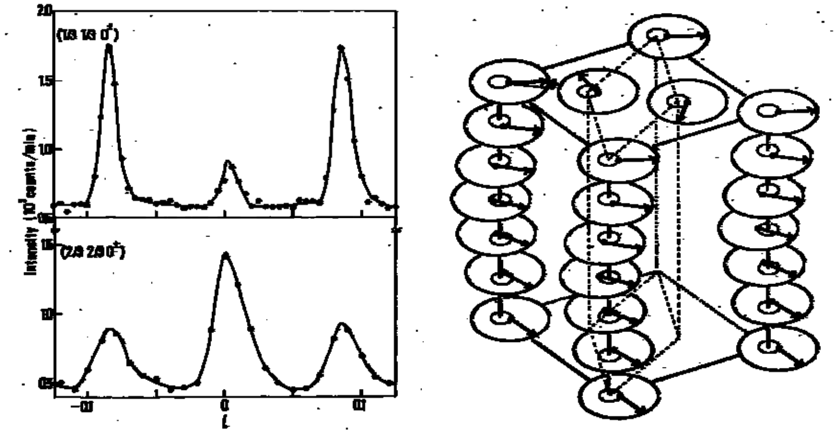

μ =0.58 (1), pitch angle = 5° (K. Adachi *et al*.)

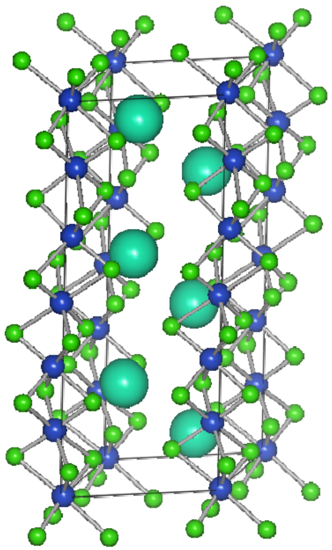

Left-handed: $P6_122$

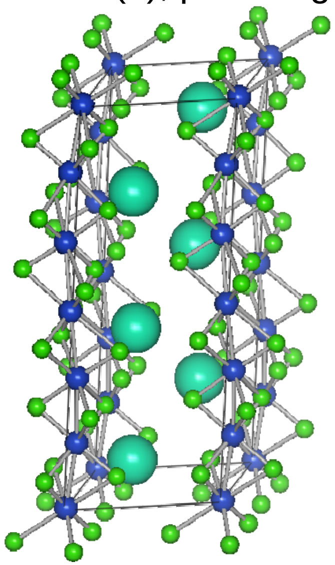

Right-handed: $P6_522$

How to Observe Crystallograhic Chirality

- Determination of Crystallographic Chirality
  - Intensities of Cu^{2+} *K*-edge in $(0,0,6n\pm2)$ with SG: $P6_122$

$$\begin{cases} I = 9\left(1+\sin^2\theta\right)\left(f_{//}-f_{\perp}\right)^2 \dfrac{\sin^2 2\alpha}{4}\left(1+\sin^2\theta\right)\left(1\pm\sin\theta\right)^2 & (l=6n-2) \\ I = 9\left(1+\sin^2\theta\right)\left(f_{//}-f_{\perp}\right)^2 \dfrac{\sin^2 2\alpha}{4}\left(1+\sin^2\theta\right)\left(1\mp\sin\theta\right)^2 & (l=6n+2) \end{cases}$$

  - Intensities of Cu^{2+} *K*-edge in $(0,0,6n\pm2)$ with SG: $P6_522$

$$\begin{cases} I = 9\left(1+\sin^2\theta\right)\left(f_{//}-f_{\perp}\right)^2 \dfrac{\sin^2 2\alpha}{4}\left(1+\sin^2\theta\right)\left(1\mp\sin\theta\right)^2 & (l=6n-2) \\ I = 9\left(1+\sin^2\theta\right)\left(f_{//}-f_{\perp}\right)^2 \dfrac{\sin^2 2\alpha}{4}\left(1+\sin^2\theta\right)\left(1\pm\sin\theta\right)^2 & (l=6n+2) \end{cases}$$

Asymmetric peak intensities are flipped by circularly-polarization and crystallographic chirality

How to Observe Crystallograhic Chirality

- Determination of Crystallographic Chirality
  - Intensities of Cu^{2+} *K*-edge in $(0,0,6n\pm2)$ with SG: $P6_122$

• Right-handed circular-polarization • Left-handed circular-polarization

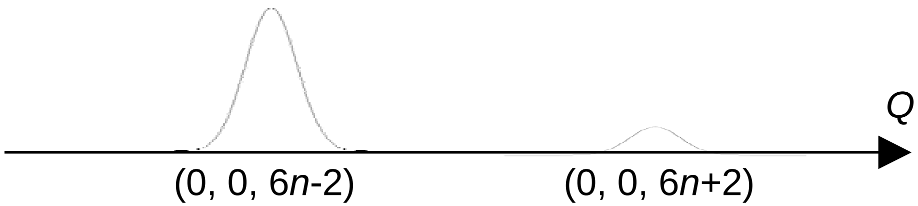

  - Intensities of Cu^{2+} *K*-edge in $(0,0,6n\pm2)$ with SG: $P6_522$

• Right-handed circular-polarization • Left-handed circular-polarization

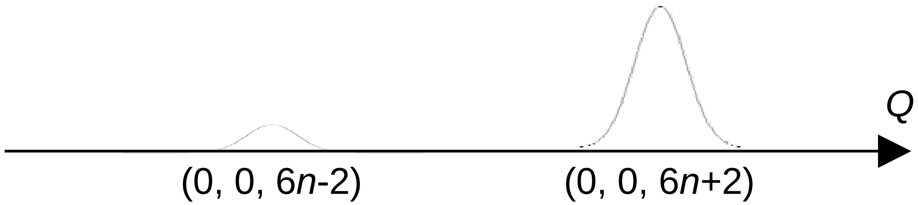

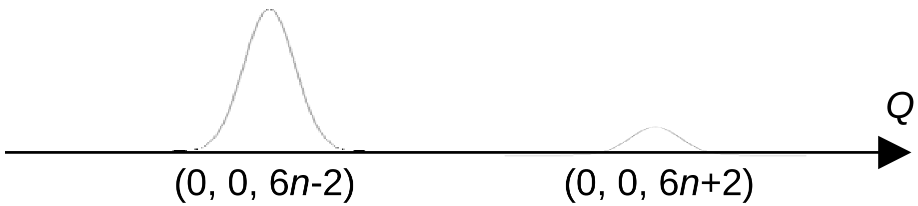

Asymmetric peak intensities are flipped by circularly-polarization and crystallographic chirality

Aoyama-Gakuin University

Summary

- Resonant Circularly-polarized X-ray Diffraction
  - We succeeded in detecting crystallographic chirality in $CsCuCl_3$
    - Asymmetric peak intensities were detected between (0,0,6n-2) and (0,0,6n+2)
    - Asymmetric peak intensities were flipped by the change of circularly polarization.
    - Asymmetric peak intensities were also flipped by the change of crystallographic chirality.

Specific heat

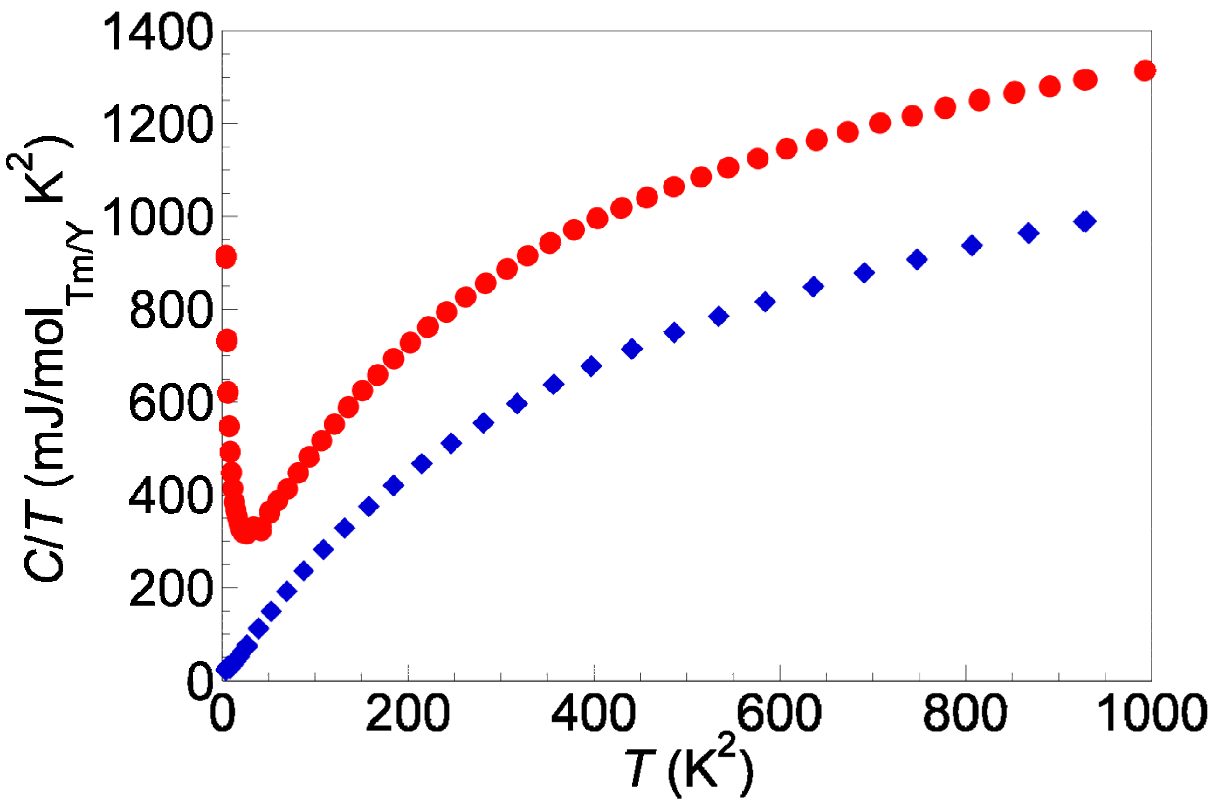

γ_{Tm} = 250 mJ/mol$_{Tm}$ K^2

γ_{Y} = 3.0 mJ/mol$_{Y}$ K^2

The anomaly (T_M) occurs around 6 K.

The very large Sommerfeld coefficient γ_{Tm} was observed.

$Tm_5Rh_6Sn_{18}$ can be categorized as a "heavy fermion superconductor".

mSR measurement 1

@RIKEN RAL in U.K.

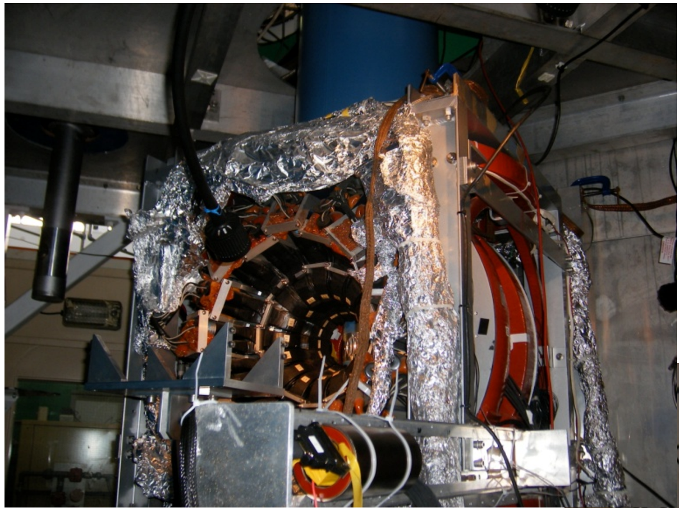

∗ RIKEN RAL
muon factory port 2

∗ Pulse muon beam

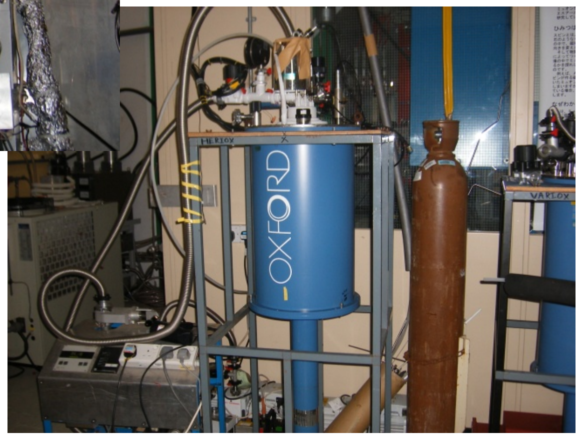

^{3}He cryostat

ZF T < 0.3 K

LF H < 4.0 kOe

sample

Ag foil, 99.998%, thin-0.1mm

Polycrystalline sample

Beam collimator, ∅ 25 mm

mSR measurement 2

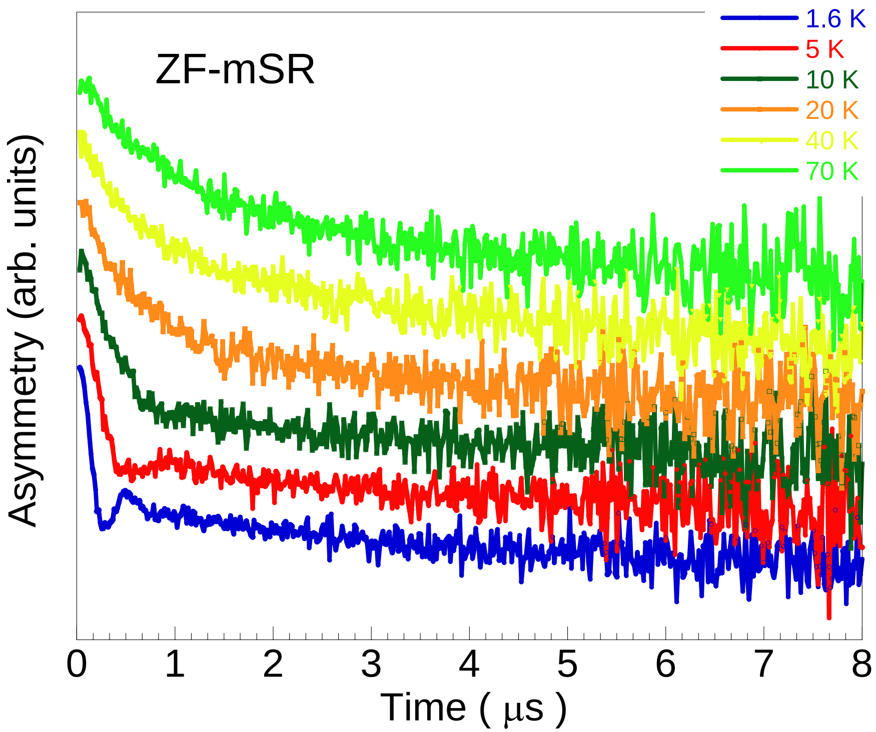

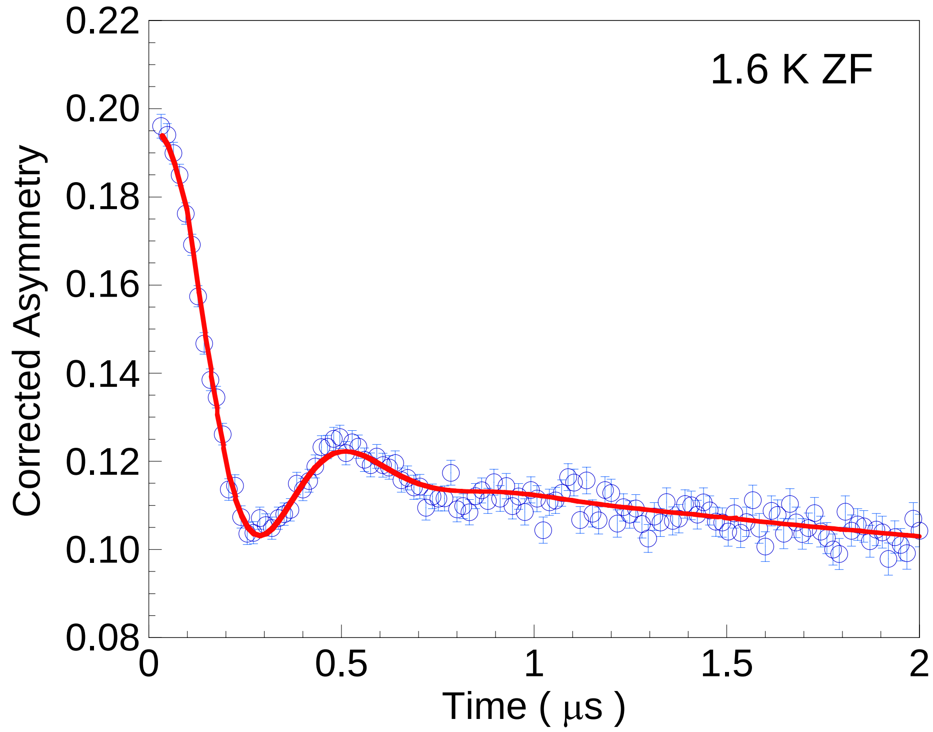

$$A_1\exp(-\lambda_1 t)\cos(f\,t + \delta) + A_2\exp(-\lambda_2 t) + A_B$$

∗ No Gaussian shape was observed above T_m

∗ Below T_m = 6 K, development of a quasi-static local magnetic field is clearly inferred from the observation of spontaneous oscillation signal in the μSR spectra.

Aoyama-Gakuin University

mSR measurement 4

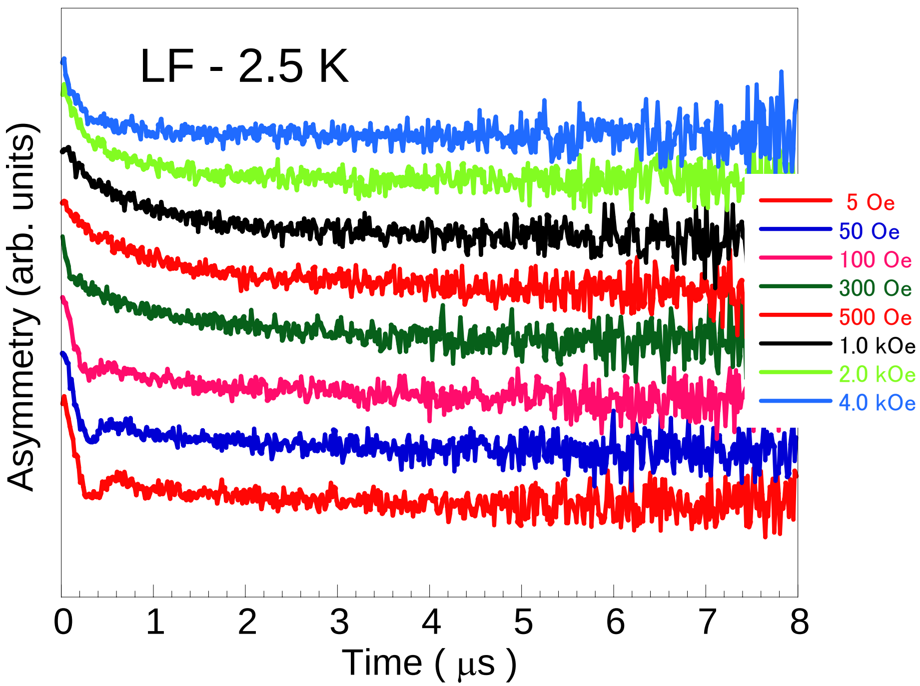

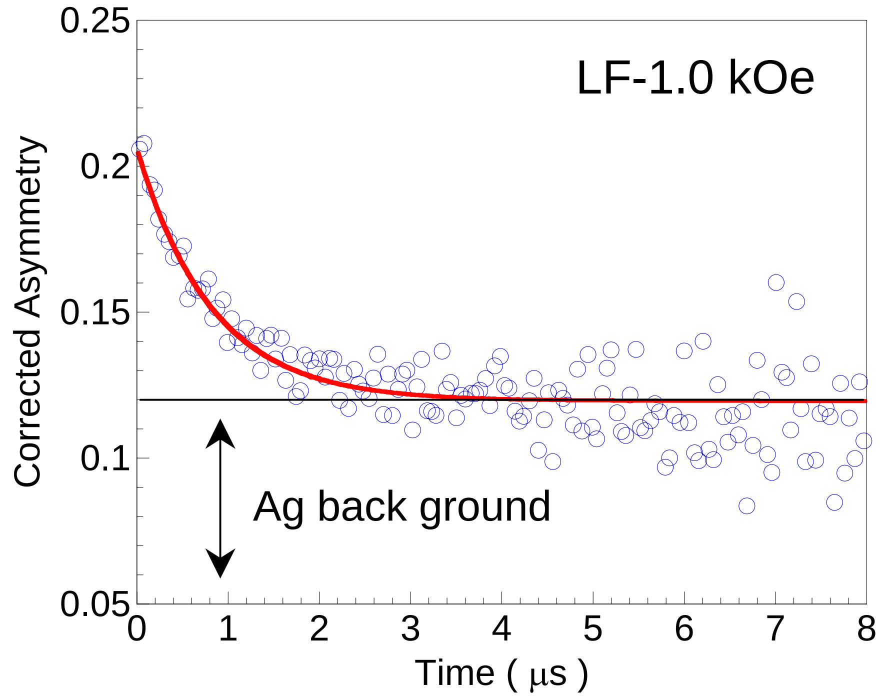

Corrected asymmetry didn't recover under strong magnetic field ($H > H_{int}$).

∗ Internal magnetic field, H = 170 Oe

Spin dynamics exists.

Detailed analysis of LF-μSR measurements is currently in progress.

Aoyama-Gakuin University

Synthesis results of $(Y,Tm)_5Rh_6Sn_{18}$

◆ $(Y,Tm)_5Rh_6Sn_{18}$ (analysis by EPMA)

$(Y_xTm_{1-x})_5Rh_6Sn_{18}$ Nominal (Y%)	$(Y_xTm_{1-x})_5Rh_6Sn_{18}$	Y contents (%)
0 ($Tm_5Rh_6Sn_{18}$)	—	**0**
10	$(Y_{0.06}Tm_{0.94})_{5.1}Rh_6Sn_{18.8}$	**6**
20	$(Y_{0.14}Tm_{0.86})_{4.9}Rh_6Sn_{18.6}$	**14**
30	$(Y_{0.20}Tm_{0.80})_{5.0}Rh_6Sn_{18.7}$	**20**
40	$(Y_{0.32}Tm_{0.68})_{4.9}Rh_6Sn_{18.7}$	**32**
50	$(Y_{0.40}Tm_{0.60})_{4.9}Rh_6Sn_{18.7}$	**40**
60	$(Y_{0.48}Tm_{0.52})_{4.9}Rh_6Sn_{18.6}$	**48**
80	$(Y_{0.72}Tm_{0.28})_{4.8}Rh_6Sn_{18.6}$	**72**
100 ($Y_5Rh_6Sn_{18}$)	—	**100**

Superconductivity in $(Y,Tm)_5Rh_6Sn_{18}$

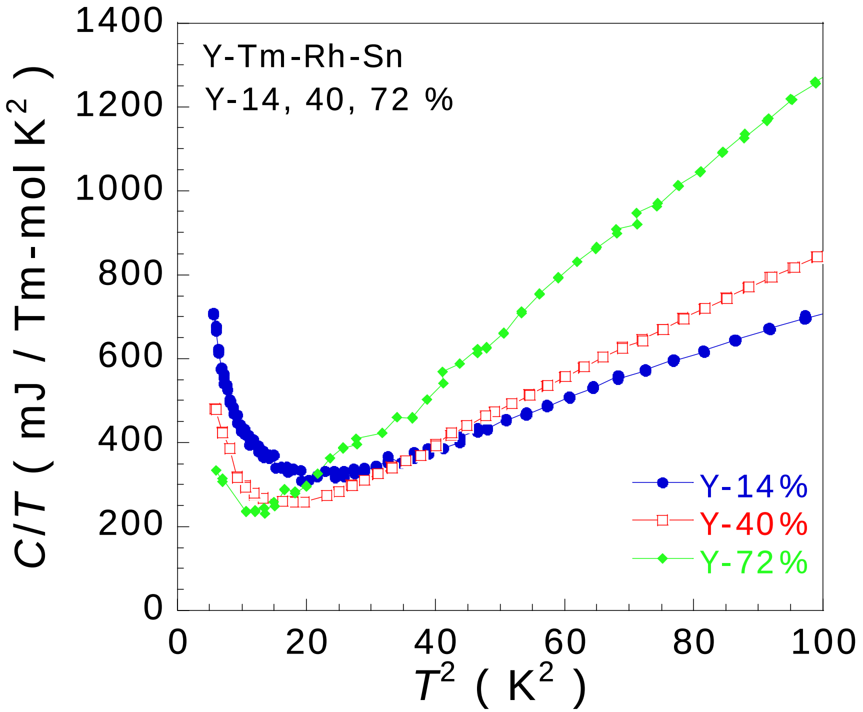

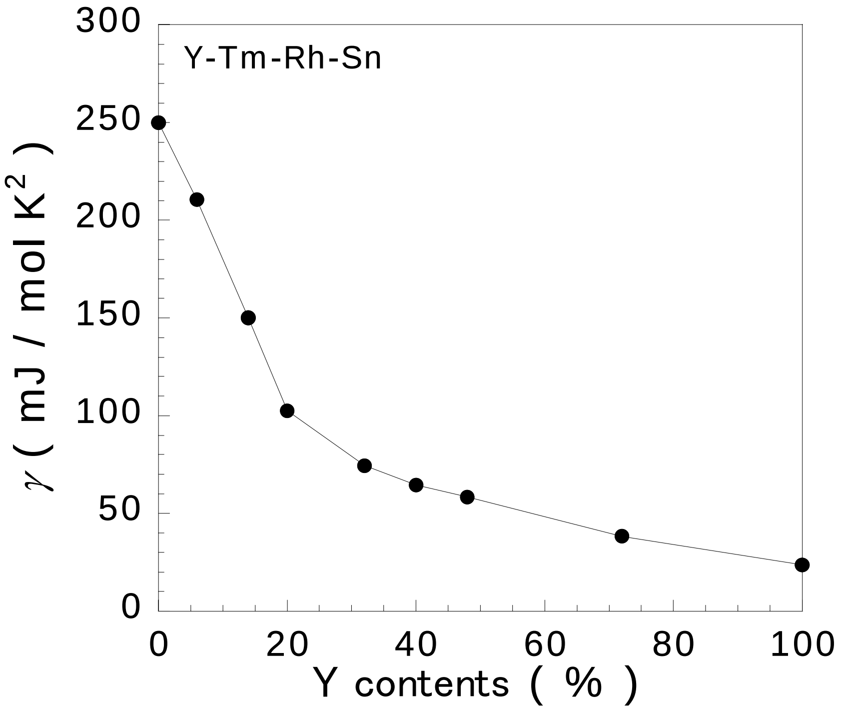

- Heavy electron state in $Tm_5Rh_6Sn_{18}$ is decreased by Y-doping.

Conclusion

∗From specific heat measurements, the reentrant superconductor $Tm_5Rh_6Sn_{18}$ can be categorized as a "heavy fermion superconductor".

∗The μSR measurement shows developmentof a quasi-static local magnetic field is clearly inferred from the observation of spontaneous oscillation signal in the μSR spectra under zero external field, where the magnetism persists even below T_c.

Strongly suggesting coexistence of magnetism and superconductivity

∗Corrected asymmetry didn't recover under strong magnetic field ($H > H_{int}$), spin dynamics exits.

Superconductivity in MgB_2

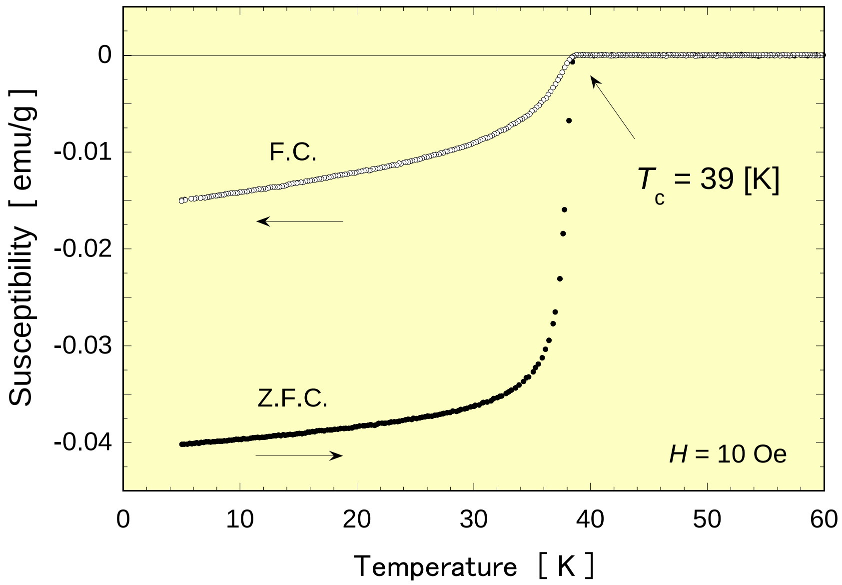

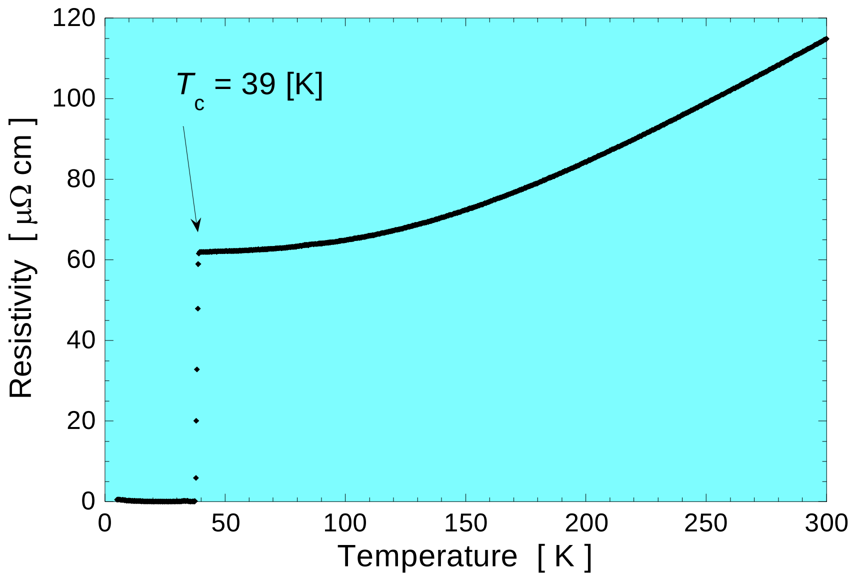

Superconductivity in B-doped diamond

- 1^{st} report;
- E.A. Ekimov *et al*., Nature <u>428</u>, 542(2004)
  - B-doping to diamond by synthesis at 8-9GPa, 2500-2800K
  - T_c~4K , H_{c2}~3.5T
    - <u>Type-II SC</u>

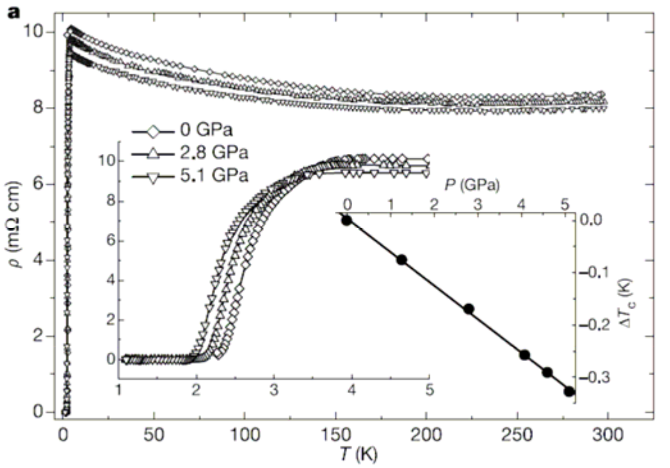

- Subsequent reports;
- Y. Takano *et al*., APL <u>85</u>, 2851(2004).
  - CVD single crystalline films
  - At same B-concentration : about $8.5\times10^{21}cm^{-3}$
    - (111)
      - T_c onset = 11.5K
    - (100)
      - T_c onset = 6.3K

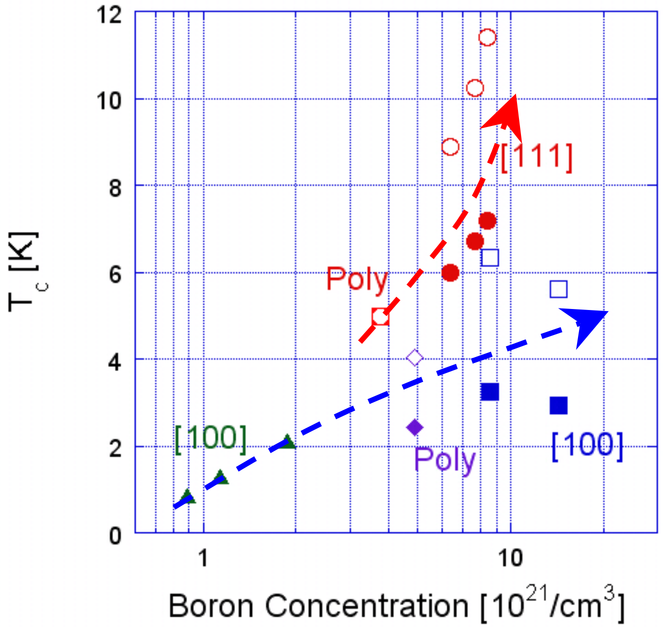

E. Bustarret et al. PRL <u>93</u>, 237005(2004).

H. Umezawa et al., cond-mat/0503303

Aoyama-Gakuin University

From real space pairing to reciprocal pairing

- Strong electron-phonon coupling leads to the insulator

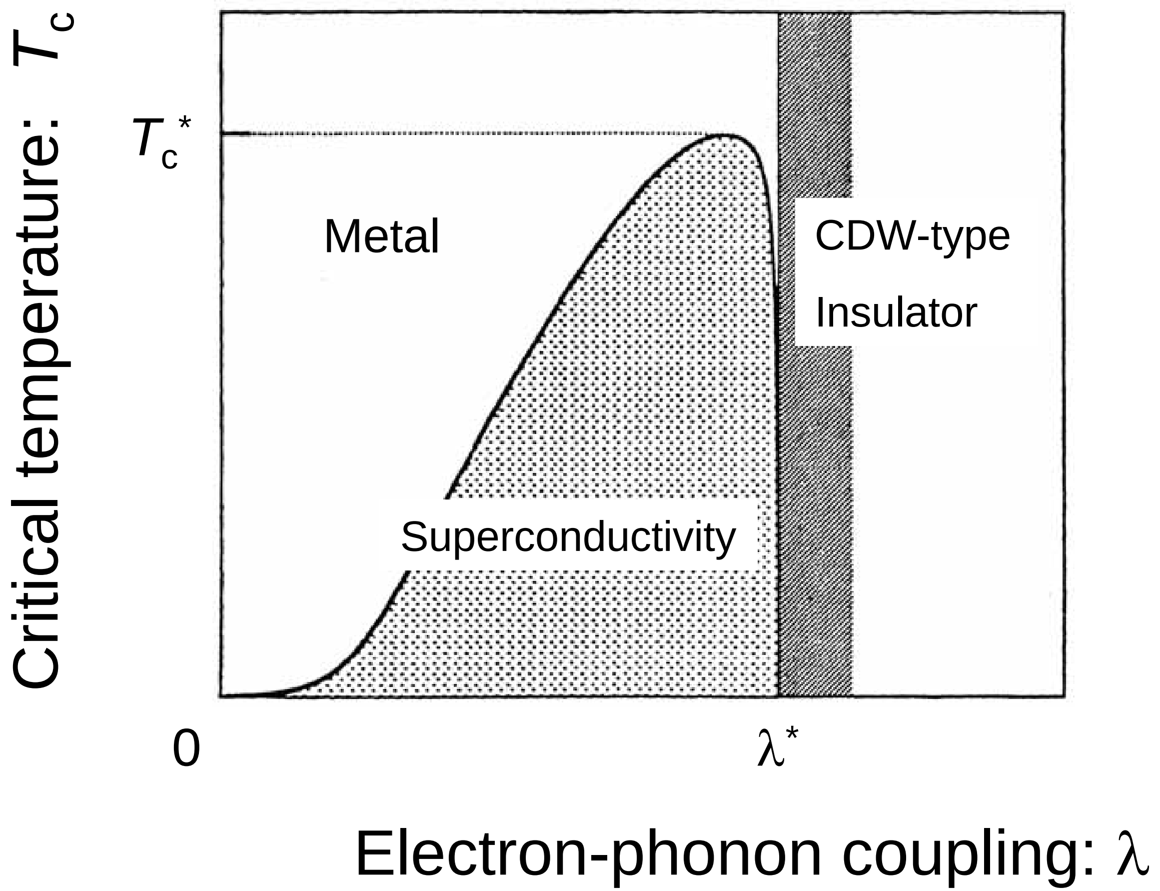

From Electro-Conductive Oxides, Tsuda, Nasu, Fujimori, Siratori

From real space pairing to reciprocal pairing

CDW（insulator）

→ **Superconductivity**

- $Ba_{1-x}K_xBiO_3$
- $BaPb_{1-x}Bi_xO_3$
- $(K_{1-x}Ba_x)_{0.3}MoO_3$
- $(Nb_{1-x}Ta_x)Se_3$

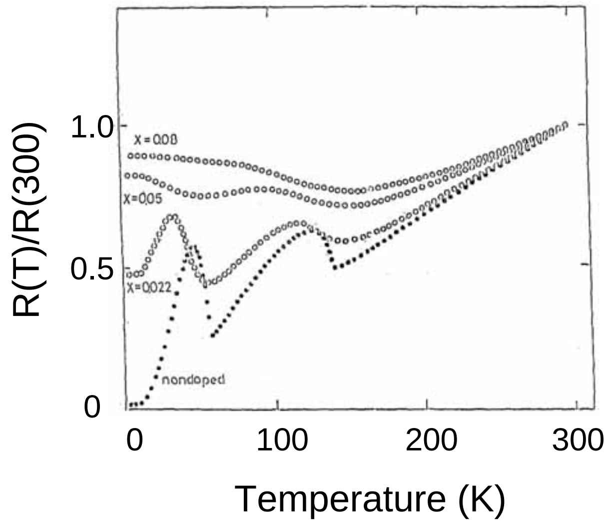

●Saito *et al*.

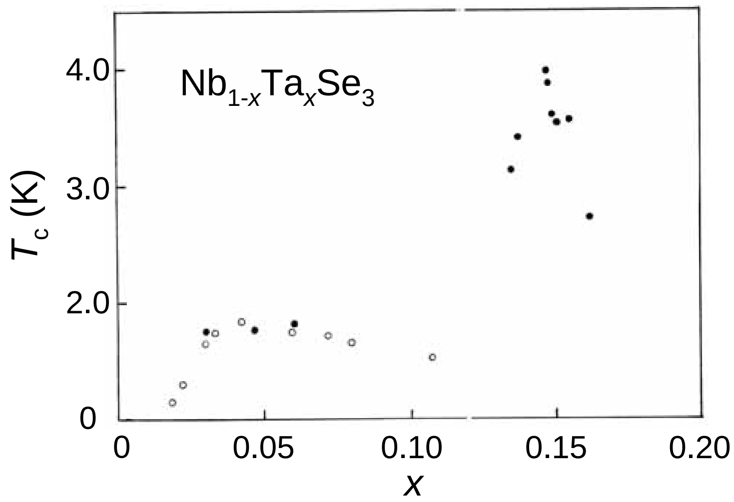

New superconductor was realized by weakening the electron-phonon interaction.

Aoyama-Gakuin University

In a previous repot

ex. $Ag_6O_8AgNO_3$

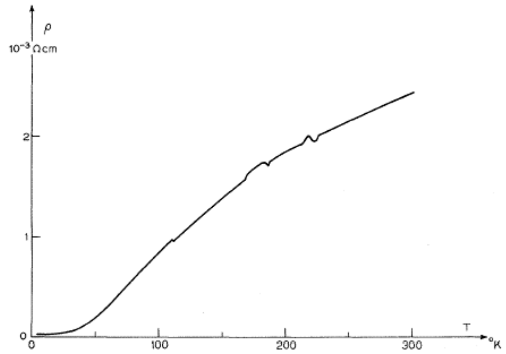

FIG. 1. The temperature-resistivity curve for a single crystal of $Ag_7O_8NO_3$.

$Ag_6O_8AgNO_3$ shows multi phase-transitions with decreasing temperature.

Robin and co-workers suggested that these transitions were generated with the structural-phase transitions.

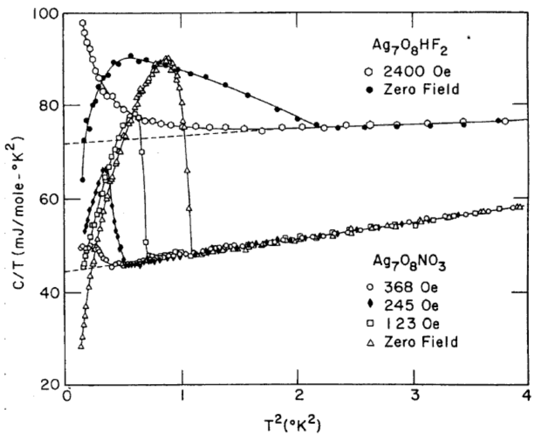

$Ag_6O_8AgNO_3$ shows superconductivity at 1.04 K

[4] M. B. Robin *et al*., Phys. Rev. Lett. **17** (1966) 917.

[5] M. M. Conway et al,. J. Phys. Chem. Sol. **31** (1970) 2673

Powder X-ray diffraction patterns of Ag_6O_8AgX ($X=NO_3$, HF_2)

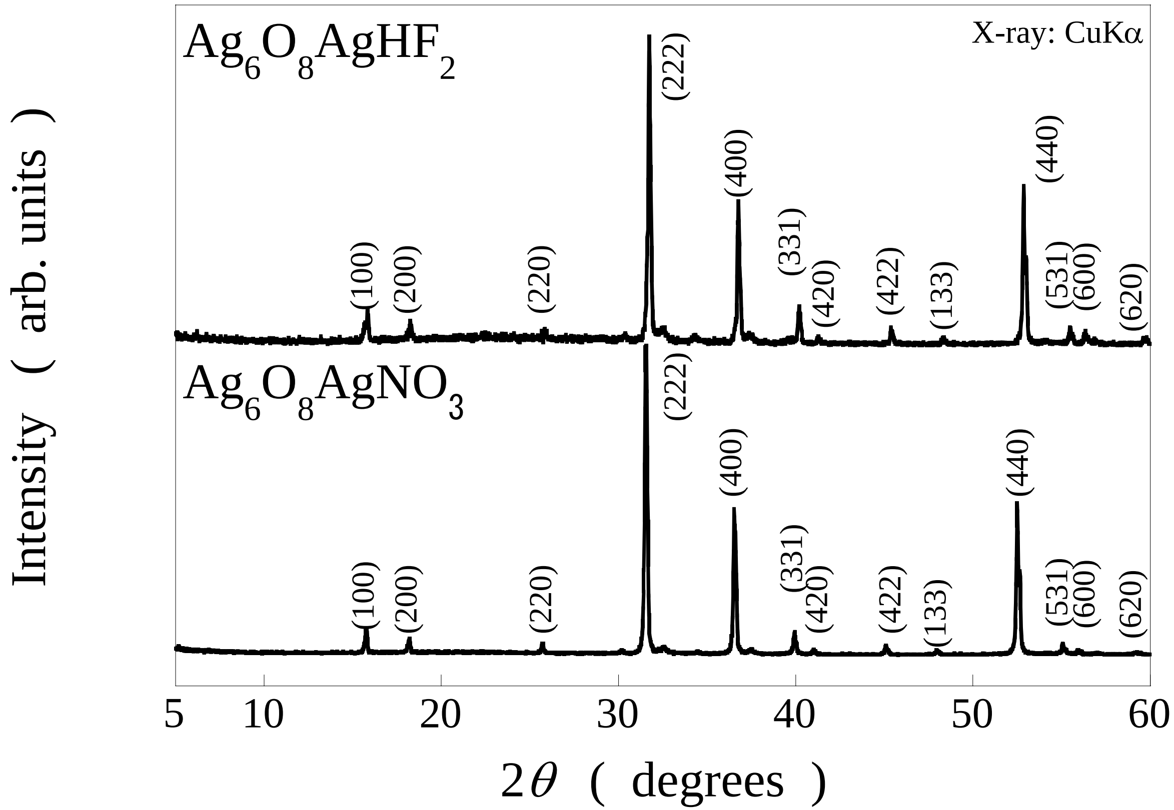

Single crystalline samples.

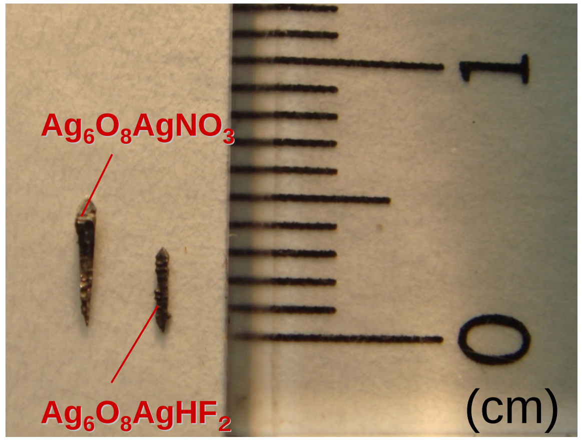

We succeeded in synthesizing single crystalline samples of $Ag_6O_8AgNO_3$ and $Ag_6O_8AgHF_2$.

Aoyama-Gakuin University